A Study on Distributed Energy Resource Management for Grid-interactive Efficient Buildings

Submitted to
Graduate School of Information Science and Technology
Osaka University

January 2024

Kenshiro KATO

Publications

Journal Article (Refereed)

[J1] Kenshiro Kato, Daichi Watari, Ittetsu Taniguchi, and Takao Onoye, “EV Aggregation Framework for Spatiotemporal Energy Shifting to Reduce Solar Energy Waste,” *IEICE Transactions on Fundamentals of Electronics, Communications and Computer Sciences*, vol. E106-A, no. 1, pp. 54-62, 2023.

[J2] Koki Iwabuchi, Kenshiro Kato, Daichi Watari, Ittetsu Taniguchi, Francky Catthoor, Elham Shirazi, and Takao Onoye, "Flexible Electricity Price Forecasting by Switching Mother Wavelets Based on Wavelet Transform and Long Short-Term Memory," *Energy and AI*, vol. 10, no. 100192, 2022.

International Conference Papers (Refereed)

[I1] Kenshiro Kato, Koki Iwabuchi, Daichi Watari, Dafang Zhao, Hiroki Nishikawa, Ittetsu Taniguchi, and Takao Onoye, “Exploring Models of Electricity Price Forecasting: Case Study on A FCAS Market,” in *Proceedings of the 5th ACM International Workshop on Applied Machine Learning for Intelligent Energy Systems (AMLIES)*, pp. 115–119, 2023.

[I2] Naoya Kaneko, Koki Iwabuchi, Kenshiro Kato, Daichi Watari, Dafang Zhao, Ittetsu Taniguchi, Hiroki Nishikawa, and Takao Onoye, “An Evaluation of Electricity Demand Forecasting Models for Smart Energy Management Systems,” in *Proceedings of the 19th International SoC Design Conference (ISOCC)*, pp. 195-196, 2022.

[I3] Kenshiro Kato, Daichi Watari, Dafang Zhao, Hiroki Nishikawa, Ittetsu Taniguchi, and Takao Onoye, “Scheduling for Multiple HVAC Systems with Electrical Power Allocation,” in *Proceedings of the 2022 IEEE 11th Global Conference on Consumer Electronics (GCCE)*, pp. 231–232, 2022.

[I4] Koki Iwabuchi, Kenshiro Kato, Daichi Watari, Ittetsu Taniguchi, Francky Catthoor, and Takao Onoye, “Demand-Aware Electricity Price Prediction Based on LSTM and Wavelet Transform,” in *Proceedings of the 38th European Photovoltaic Solar Energy Conference and Exhibition (EUPVSEC)*, 7DV.1.4, pp. 1668-1670, 2021. (Poster Award Winners)

[I5] Kenshiro Kato, Daichi Watari, Ittetsu Taniguchi, and Takao Onoye, "A Framework on Spatiotemporal Shifting of Solar Energy Based on EV Aggregator," in *Proceedings of the 36th European Photovoltaic Solar Energy Conference and Exhibition (EUPVSEC)*, 6CV.1.16, pp. 1877–1880, 2019.

Summary

The drive toward a low-carbon society and the urgent need to address energy issues have gained increasing prominence in recent years, as evidenced by the United Nations Sustainable Development Goals. This global shift underscores the critical necessity of transitioning to sustainable energy systems, particularly in the face of challenges such as climate change and energy scarcity. The adoption of renewable energy sources, notably solar and wind power, is playing a pivotal role in paving the way for this sustainable future. Data from the last few decades shows a consistent and impressive growth in the worldwide capacity of renewable energy installations. Despite their environmental benefits, renewable energy sources present significant challenges for the capacity and stability of electricity grids. Their output is inherently inconsistent and subject to fluctuations due to environmental factors like weather and wind speed, and lacks the controllability characteristic of traditional power stations. Such variability in renewable energy production can lead to substantial issues in grid stability, including frequency fluctuations, grid line overloads, and imbalances between supply and demand. To compensate for the unpredictability of renewable energy outputs, there is a growing need for measures such as adjusting generation levels and utilizing energy storage systems. These interventions are essential to ensure a reliable and efficient integration of renewable energy into the power system.

Addressing these challenges, grid-interactive efficient buildings (GEBs) have emerged as a key solution. Defining by the U.S. Department of Energy, GEBs are energy-efficient buildings that use smart technologies and on-site distributed energy resources (DERs) to provide demand flexibility. The international energy agency (IEA) also has a similar definition. They co-optimize for energy cost, grid services, and occupant needs and preferences in a continuous and integrated manner. GEBs are becoming pivotal in enhancing the affordability and reliability of power systems in the U.S., significantly contributing to the reduction of greenhouse gas emissions by reducing overall energy consumption and enhancing demand flexibility. This is crucial for the seamless integration of renewable energy sources into the grid. GEBs offer direct benefits to consumers, such as reduced system costs and enhanced demand flexibility, leading to lower electricity bills and reduced consumption. They also improve the reliability of the system and increase the satisfaction of building owners and occupants by providing more options, resilience, and flexibility in terms of electricity consumption. The multifaceted

benefits of GEBs highlight their essential role in transforming the energy landscape and enhancing consumer experiences and sustainability.

This dissertation delves into several key aspects of GEBs, focusing on load shedding, load shifting, and generation. These areas are where significant improvements can be achieved through information technology links. In this dissertation, research will be conducted on the generating and consuming sides to improve these strategies. This dissertation excludes considerations such as battery storage modeling and renewable energy production. Furthermore, the participation of GEBs in demand response and balancing markets, where electrical flexibility is dealed, is integral to the modern energy ecosystem. By actively participating in these markets, GEBs can capitalize on their ability to dynamically adjust energy consumption and production in response to real-time market signals. Thus, GEBs potentially contribute to several important aspects of grid stability and maximize their economic returns. This dissertation therefore addresses the following points, aiming to improve their effectiveness and further challenge efficient market participation.

- How to maximize the potential of renewable generation.
- How to manage DERs such as air conditioning systems for modifying load profile.
- How to effectively get rewards through flexibility market participation.

Within the broader scope of GEBs and DERs management, particularly photovoltaic (PV) generation, strategic planning is crucial for evaluating GEB performance and estimating long-term electrical costs. However, the typical method of selling excess solar energy via reverse power flow often leads to instability in the power system. In this context, the role of electric vehicles (EVs) becomes pivotal in effectively utilizing and reducing solar energy waste by filling the spatiotemporal gap in solar energy. This dissertation proposes a novel EV aggregation framework for the spatiotemporal shifting of solar energy, reducing the need for reverse power flow. This framework can contribute to reducing solar energy waste by manipulating pricing strategies for charging and discharging via an EV aggregator. The proposed EV aggregation enables EVs to spatiotemporal shift energy from building to building. Simulation results demonstrate a substantial reduction in solar energy waste, up to 68%, using this novel framework.

Significant research in GEBs focuses on GEB load shedding and shifting strategies through various DERs, particularly HVAC systems. HVAC is crucial due to its high demand within buildings and existing installations, reducing additional costs. This dissertation optimizes HVAC operations by allocating electrical power based on occupancy and outdoor unit capacity, ensuring that the total power consumption complies with peak demand limitations. Various methods, including model predictive control (MPC) and reinforcement learning, are explored for HVAC scheduling. While MPC is effective in long-term planning, its computation time increases with more units, and reinforcement learning requires extensive data and struggles with comfort uncertainty. This dissertation presents a solution that efficiently meets power constraints across multiple units without violating power limitations or sacrificing thermal comfort. The proposed method, balancing electricity costs and thermal comfort through multi-objective optimization, demonstrates that the scheduling of multiple HVAC systems can be achieved efficiently. By integrating the proposed methodology with appropriate HVAC aggregation techniques, a comprehensive framework for energy management in buildings can be provided.

GEBs have evolved from passive power consumers to active participants in the electricity supply and demand balancing market, playing a key role in efficiently integrating renewable energy sources like solar and wind power. This integration is crucial for managing energy variability and preventing grid overloads during peak times. A critical aspect of GEBs' effective market participation involves accurately predicting market transaction prices. This capability is essential for optimizing energy buying or selling strategies, maximizing revenue, and developing efficient energy supply approaches. In this context, the dissertation introduces a novel market price forecasting model tailored for the frequency control ancillary service markets. This model, derived from wholesale market data and considering varying response times, significantly improves the accuracy of the prediction. Experimentally, it has been shown to reduce the root mean square error by 80% compared to existing forecasts from the Australian energy market operator, indicating its effectiveness in supporting the strategic participation of GEBs in energy markets.

Acknowledgments

First and foremost, I extend my sincere appreciation and heartfelt thanks to my supervisor Associate Professor Ittetsu Taniguchi, Department of Information Systems Engineering, Graduate School of Information Science and Technology, Osaka University. He exemplified what exceptional supervisors do, guiding and supporting in ways that profoundly shape their mentees. Without his generous support, I wouldn't have become who I am today, nor would I be leading the life I now cherish. His insightful guidance and unwavering support were instrumental in achieving the advanced outcomes of my research.

I express my gratitude to Professor Takao Onoye from the Department of Information Systems Engineering at the Graduate School of Information Science and Technology, Osaka University, for his insightful feedback and valuable advice. His expert perspectives were crucial, and I am greatly indebted to him for his meticulous and insightful guidance throughout this research.

My profound thanks go to Professor Francky Catthoor from the Department of Electrical Engineering (ESAT) at KU Leuven and an imec fellow. His priceless guidance and suggestions significantly contributed to my research. He consistently encouraged collaboration with EnergyVille and NTUA/AUTH colleagues, as well as interaction with experts in related fields. His support was a fundamental element in the extensive development of this dissertation. Additionally, his support was invaluable during my stay at EnergyVille, Belgium, greatly impacting both my professional journey and personal life.

My sincere thanks are extended to Professor Noriyuki Miura from the Department of Information Systems Engineering at the Graduate School of Information Science and Technology, Osaka University. His meticulous reviews and perceptive recommendations have significantly influenced the direction of my dissertation, steering it towards improved and innovative pathways.

I extend my gratitude to Assistant Professor Hiroki Nishikawa, Department of Information Systems Engineering, Graduate School of Information Science and Technology, Osaka University. His invaluable advice and extensive assistance have been pivotal in my academic journey. I have greatly benefited from his profound insights into research methodologies and his constructive critiques.

I express my sincere gratitude to Assistant Professor Dafang Zhao, Department of

Information Systems Engineering, Graduate School of Information Science and Technology, Osaka University. Throughout my doctoral journey, the support I received from him, ranging from regular research and thesis writing to managing lab operations, has been invaluable. His presence has been of paramount importance throughout my doctoral journey.

My acknowledgment extends to the team at imec for their integral role in time series data forecasting. Special thanks are due to Assistant Professor Patrizio Manganiello from the Department of Electrical Sustainable Energy at TU Delft. His astute counsel during our meetings, and his contributions to various aspects of the research, such as documentation, code validation, and literature review, were indispensable. I am convinced that this project would not have reached its current stage without his involvement.

I am grateful to Professor Yoshiyuki Shimoda in the Division of Sustainable Energy and Environmental Engineering at the Graduate School of Engineering, Osaka University, for introducing me to the core concept of this research, grid-efficient interactive building. I extend my sincere thanks to Associate Professor Toshihiro Suzuki in the Campus Sustainability Office, Osaka University, not only for his regular guidance in my research but also for his invaluable advice in shaping my future career path. My gratitude extends to Assistant Professor Hideaki Uchida in the Division of Sustainable Energy and Environmental Engineering at the Graduate School of Engineering, Osaka University. Appreciation is also due to the employees of DAIKIN Industries, Ltd., Mr. Sumio Shiochi, Mr. Shinya Harada, Mr. Masakazu Okamoto, Mr. Yoshinori Yura, Mr. Minoru Tomoda, Mr. Yasuhiro Sugimoto, and Mr. Shuuichi Kurose for their invaluable input and extensive support in the on-site HVAC experiment of another project.

I express my heartfelt thanks to all members of the Onoye Laboratory for the enriching and enjoyable experiences shared. Special appreciation goes to Mrs. Yuki Yoshida, the secretary of Onoye Laboratory, whose support was pivotal in my lab life, allowing me to focus deeply on my research. I am extremely grateful to Dr. Daichi Watari, an alumnus of the Onoye Laboratory. His support extended beyond research assistance and guidance in lab life. More importantly, I am thankful for his pioneering journey into the doctoral program, paving the way for juniors like me. His example inspired my decision to pursue a doctorate, playing an important role in shaping who I am today. Additionally, I am grateful to the members of Group CPS, Ms. Theint Theint Thu, Mr. Yuki Ozawa, Mr. Koki Iwabuchi, Mr. Shotaro Nonaka, Mr. Naoya Kaneko, Mr. Shunsaku Miyatake, Mr. Kazuki Okazawa, Mr. Shuhei Mitsunaga, and Mr. Ren Sasaki. Their feedback and insights during meetings have been invaluable, and the enjoyable moments shared with them have been a source of constant motivation. I would also like to express my gratitude to my alumnus colleague from the laboratory, Mr. Takuya Jikan, Mr. Yuta Kawasaki, Mr. Mitsuhiro Kawasaki, Mr. Kento Nishikawa, Ms. Saya Suzunaga. Their support and camaraderie during our time together were invaluable.

I want to express my deepest gratitude to all the friends who have maintained our friendship unchanged even after graduation. I am especially grateful to Mr. Masaki

Tokai and Mr. Kazutaka Yoneda. Your willingness to continue our fun times together has been a great source of comfort and support for me. Additionally, I extend my thanks to everyone involved with the Osaka University American Football Team, the Tridents. Being part of this team has been a crucial factor in my personal growth, and I am grateful for the experiences and lessons learned.

My profound gratitude is directed towards my family: Mr. Takeshi Kato, Mrs. Akemi Kato, Mrs. Miyu Kato, and Mr. Daiki Kato. Your unwavering love and patience are the pillars of my strength every day. The completion of this journey would have been impossible without the steadfast support of my family.

Contents

List of Figures

List of Tables

Chapter 1

Introduction

1.1 Background

Nowadays, the drive toward establishing a low-carbon society and addressing energy issues has become increasingly pronounced. As noted in the United Nations Sustainable Development Goals Report [1], the convergence of global challenges, including climate change and energy scarcity, underscores the critical need for the transition to sustainable energy systems.

There has been a noticeable increase in the adoption of renewable energy to pave the way for a sustainable future [2,3]. This trend is shown in Figure 1.1, where data indicate a consistent increase in the worldwide capacity of renewable energy installations over the last several decades [4, 5]. Specifically, from 2006 to 2022, there has been an impressive growth in wind and solar energy capacities, which have increased by 825 GW and 1046 GW, respectively. These sources of renewable energy are also appealing from a sustainability point of view, as they generate clean energy with no CO_2 emissions and reduce the dependence on exhaustible fossil fuels.

Despite the environmental benefits of renewable energy, it presents considerable challenges concerning the capacity and stable operation of electricity grids [6]. The output of renewable sources is frequently inconsistent and fluctuates based on environmental factors such as wind speed, solar exposure, and cloud cover. Moreover, their generation cannot be controlled in the same manner as conventional power stations, such as coal plants, which can be adjusted up or down, or switched on or off, as needed. These fluctuations in renewable energy production can lead to significant issues with grid stability, including frequency fluctuations, grid line overloads, and imbalances between supply and demand [7]. To address these grid stability issues, ancillary services have become increasingly important. These services provide essential support to the grid, including frequency regulation, voltage control, and emergency backup, helping to manage the imbalances and ensure a reliable electricity supply. The grid is thus under strain from the swift incorporation of renewable sources. To manage this variability,

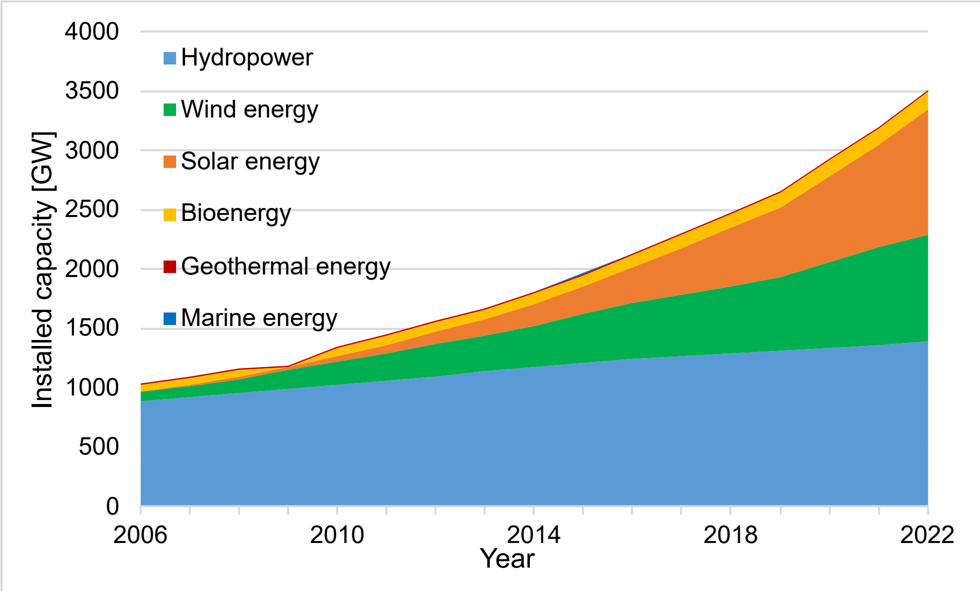

Figure 1.1: Installed global renewable energy capacity by technology

supply-side utilities must maintain a balance between supply and demand using their generation systems [8]. This includes preparing for power fluctuations by constructing new power stations and updating existing ones. Nonetheless, maintaining large-capacity power plants that are rarely utilized is not cost-effective. Therefore, alongside supply-side solutions, leveraging demand-side energy resources has become increasingly important.

Buildings are major energy consumers that impose tremendous strain on the modern grid. This trend is depicted in Figure 1.2, where data indicate that the global shares of final energy in buildings are 36% and 37% [9, 10]. There exists a potential for them to play a pivotal role in balancing the supply and demand of the grid. By integrating smart systems and energy storage solutions, buildings can respond effectively to fluctuations in renewable energy supply, thus contributing to grid stability. Such strategies could alleviate the need for large-capacity power plants, which are not cost-effective. In response to these opportunities, the concept of grid-interactive efficient buildings (GEBs) has been proposed.

The U.S. department of energy (DOE) defines GEBs as an energy-efficient building that uses smart technologies and on-site distributed energy resources (DERs) to provide demand flexibility while co-optimizing for energy cost, grid services, and occupant needs and preferences, in a continuous and integrated way [11]. The IEA reported recommendations and guidelines for the realization of GEBs [12]. This report employs a definition of GEBs similar to that used by the DOE. By doing so, GEBs have emerged as pivotal contributors to enhancing the affordability and reliability of the U.S. power system. Furthermore, GEBs play a crucial role in curbing greenhouse gas emissions by

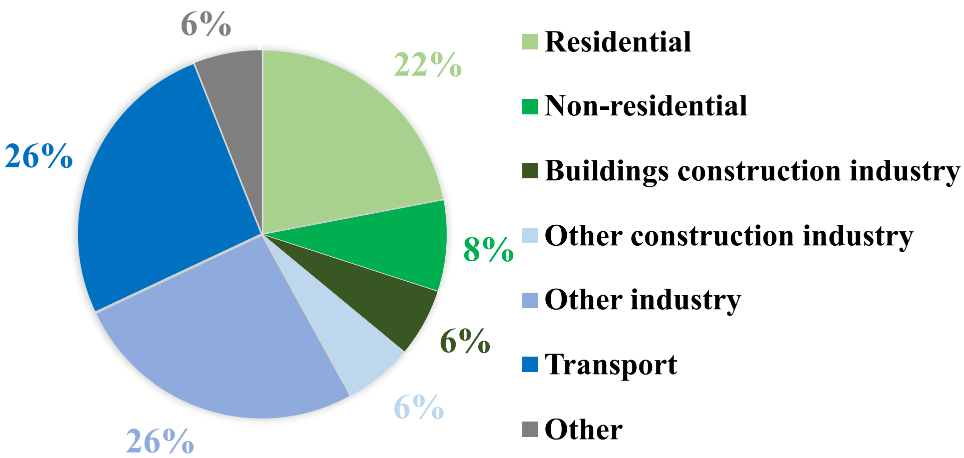

Figure 1.2: The share of global final energy consumption by buildings and construction in 2020

reducing overall energy consumption and enhancing demand flexibility, thus facilitating the seamless integration of renewable energy sources.

Figure 1.3 shows the main components of the GEB. These components include energy generation systems such as solar panels, energy storage units like batteries, and smart management systems that control and optimize energy use and DERs within the building. Importantly, GEBs offer direct benefits to consumers through DER management, such as solar panels, batteries, electric vehicles, and smart appliances. GEBs achieve this by enhancing energy efficiency and demand flexibility within buildings, which in turn contributes to the grid's stability and efficiency. Moreover, improvements in system reliability resulting from demand flexibility represent a substantial benefit to consumers. Furthermore, GEBs elevate the satisfaction of building owners and occupants by providing increased options, resilience, and flexibility in terms of electricity consumption. In certain cases, these advancements have led to an overall improvement in the comfort levels of building occupants. Such multifaceted benefits underscore the pivotal role of GEBs in not only transforming the energy landscape but also enhancing the overall consumer experience and sustainability of the built environment.

The challenge lies in the orchestration of these DERs - solar panels, batteries, electric vehicles, and smart appliances - ensuring that they operate harmoniously to balance energy supply with fluctuating demand. As outlined in the technical reports from the U.S. DOE regarding GEBs [11], there are five demand-side management strategies crucial to improving building energy efficiency and grid interaction: efficiency, load shedding, load shifting, modulating, and generation. Table 1.1 provides the detailed definitions and key characteristics for each strategy. The realization of GEBs is based on the efficient management of DERs and the sophisticated handling of information. GEBs represent a transformative approach, integrating DERs to not only improve en-

Table 1.1: Five strategies for demand-side management in GEB [13]

	Definition	Key Characteristics	Load Profiles
Efficiency	Consistent reduction in power consumption, regardless of time.	Long-term, continuous reduction.	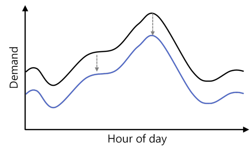
Load Shedding	Temporary decrease in power consumption during peak usage periods or in response to emergency events.	Power consumption need to be promptly decreased upon receiving signals and typically remains down for around one hour.	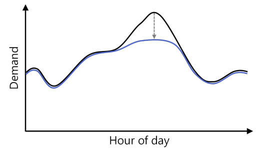
Load Shifting	The building modifies its energy usage schedule to lower power demand during peak hours or to better utilize renewable energy sources.	Power consumption need to be promptly decreased upon receiving signals and typically remains down for two to four hours.	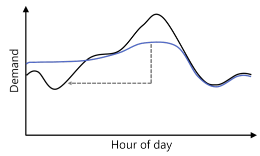
Modulate	The building automatically adjusts its power consumption in response to signals from the grid operator.	Power consumption need to be modifiable at intervals of one second or less.	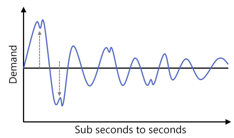
Generation	The building generates electricity for on-site use or supply to the grid during peak demand hours.	Power consumption must be promptly decreased upon getting notifications and typically lasts for two to four hours.	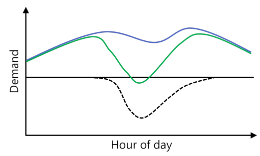

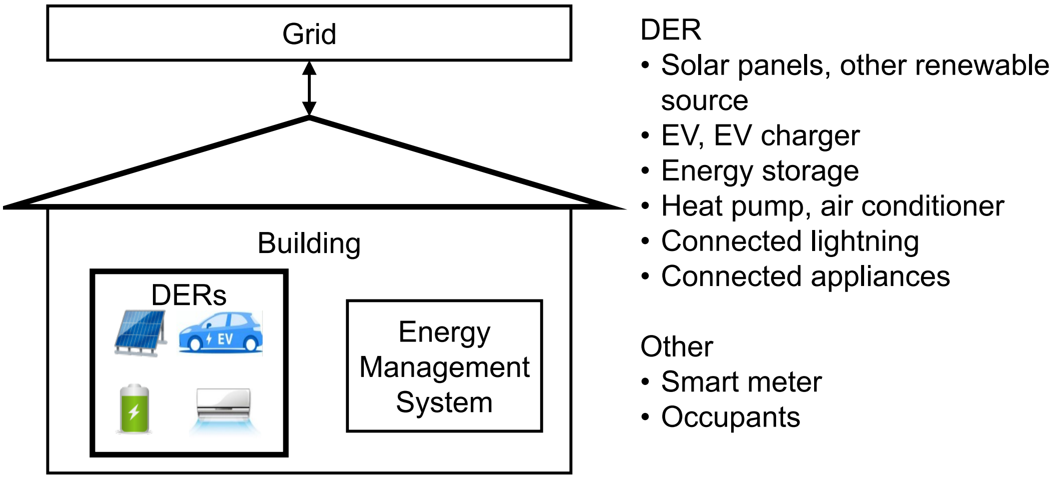

Figure 1.3: Components of a grid-interactive efficient building

ergy costs and comfort within buildings but also actively contribute to grid stability. A key aspect of effectively managing DERs is the deployment of advanced control systems that can respond dynamically to grid signals, optimize energy usage, and engage in real-time energy transactions, both within and beyond the building's parameters.

The global supply-demand balance is expected to become more complex in the future, with a shift towards renewable energy sources for power generation. Consequently, it is essential for GEBs to handle DERs with more flexibility. Specifically, the challenge lies in contributing to the power grid, such as "demand-side management strategies for GEB" and creating flexibility for supply-demand balance, without compromising the building's primary objectives, such as minimizing electricity costs and ensuring residents' comfort. Therefore, this study aims to improve the effectiveness of GEBs by addressing challenges related to load shedding, load shifting, and generation. The strategies of efficiency and modulation are outside the scope of this study, as they are mainly within the research scope of the Mechanical Engineering Research Institute. Furthermore, the participation of GEBs in demand response markets is essential for the modern energy ecosystem. By actively participating in these markets, GEBs can capitalize on their ability to dynamically adjust energy consumption and production in response to real-time market signals. Thus, GEBs contribute to grid stability and maximize economic returns. Therefore, this dissertation also challenges further efficient market participation through information technology.

To achieve this kind of energy management, this dissertation divides GEB into three key perspectives to improve its capabilities in each area. These parts are "store," "consume," and "interact." "Store" refers to how electricity generated within a GEB is stored and when it is used. The most crucial aspect of 'store' is storage, primarily using residential batteries and electric vehicles. Next, "consume" refers to when and how much various appliances are used in GEBs. Figure 1.4 demonstrates the proportion of power

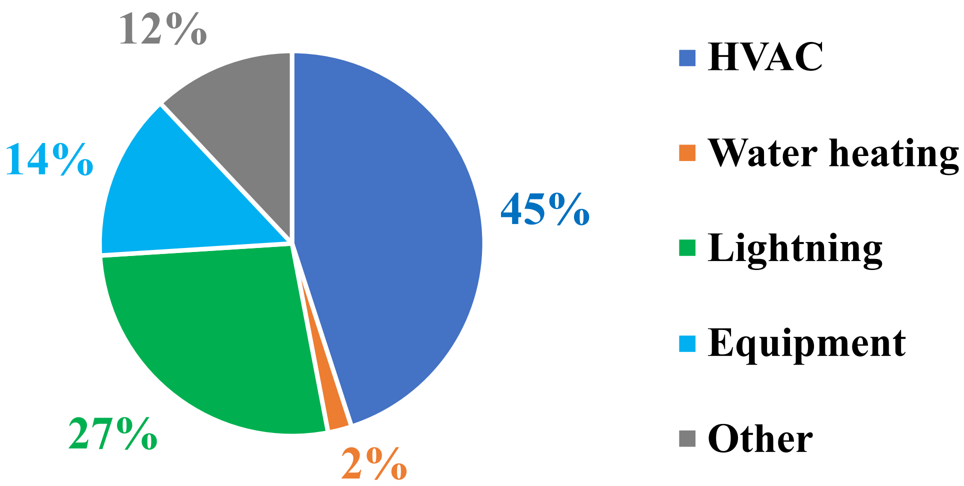

Figure 1.4: Global share of buildings and construction by end use in 2020

consumption within a building. In particular, air conditioning and lighting, which make up a significant part of the system, have the potential for substantial contributions. Finally, "interact" involves the interaction between GEBs and the grid. Traditionally, the rewards in GEBs for altering building demand were reductions in total power consumption and peak power, thus lowering electricity costs. However, in recent years, the ability to trade the potential of demand shape changes as the electrical flexibility in the market has emerged. Consequently, the interaction between the GEBs and the grid is rapidly evolving. This dissertation focuses on the following points regarding the above key points.

- Store: How to maximize the potential of renewable generation.
- Consume: How to manage DERs for GEB's load modification.
- Interact: How to effectively receive rewards through market participation.

1.2 Related Research

This section introduces research related to GEBs. First, studies on the overall concept of GEBs and the strategies that are the focus of this research are presented. Next, research on the creation of electrical flexibility through GEBs is introduced.

1.2.1 Grid-interactive Efficient Buildings

In the burgeoning field of GEBs, studies are pivotal for the evolution and implementation of these advanced systems. GEBs are advanced structures that actively manage energy consumption and generation, integrate with the power grid to optimize efficiency, reduce costs, and contribute to energy sustainability. Liu et al. [14] underscore the crucial role of GEBs in facilitating the low-carbon transition by maximizing the use of renewable energy within the building sector. This study highlights the importance of GEBs in reducing carbon emissions, aligning with global sustainability goals. Ye et al. [15] provide a foundational framework for the deployment of GEB, highlighting a structured approach that includes assumptions, modeling, and simulation to address research questions and achieve efficient problem solving strategies. In addition, the potential of GEBs to function as active elements within a microgrid is exemplified through case studies using prototype commercial building models developed by the U.S. DOE. This study [16] illustrates the integration of photovoltaic (PV) generation and energy efficiency applications, serving as a template for future GEB implementations.

Recent research about GEBs marks a shift towards dynamic energy management. Li et al. [13] focus on energy flexibility in residential buildings, highlighting its role in optimizing flexible loads and contributing to a reliable power grid. They explore electrical flexibility's applications across various scales and its essential performance metrics and control strategies. Steen's review [17] emphasizes demand-side management strategies such as load shedding, shifting, and modulation, which are crucial for balancing energy demand and supply, particularly during peak periods. These strategies, which integrate advanced technologies and smart controls, are vital to improving energy efficiency and grid stability. The following parts introduce each of these demand strategies in GEBs.

Load Shedding

Load shedding is the ability of a building to reduce electricity use during a short period, which typically occurs during times of peak demand or emergencies and on short notice. The GEB load shedding strategy is important because it helps reduce the highest energy use, ease the load on the power grid, and make energy use more efficient and stable.

Consume: One of the most significant DER devices for load shedding within GEBs is HVAC systems. The International Energy Agency has identified HVAC loads in buildings as having the greatest potential to provide grid services due to their substantial portion of the electric load and the flexibility of operation afforded by passive thermal storage of the mass of the building [10]. This trend is depicted in Figure 1.4, where data indicate that space heating and cooling power consumption accounts for about 40% of the building's power consumption [9, 10]. This is because HVAC systems can easily be turned off and the environmental changes caused by turning them off are gradual. Some studies provide a framework that includes load shedding as a core component of demand response capabilities [14, 18]. However, these studies lack consideration for the comfort of residents. Therefore, a more sensitive approach that takes into account comfort is necessary.

Store: On-site generation, particularly PV systems, and energy storage are essential in load shedding operations. Integration of these DERs enables buildings to shed loads by relying on their generated power during peak times, as shown in a detailed analysis by the Department of Energy, which uses prototype commercial building models to demonstrate this capability [16]. This method is discussed in more detail in the literature [19], with a focus on creating analytical frameworks that see buildings as flexible grid resources and include load shedding as a function of time-sensitive efficiency.

Load Shifting

Load shifting is the ability to change the time of electricity use, which is by decreasing demand during one period while increasing demand during another. The GEB load shifting strategy is essential to balance energy demand and supply by moving energy use from peak times to off-peak periods, thus enhancing grid stability and optimizing energy costs.

Consume: HVAC systems represent a substantial portion of the energy load in buildings and offer significant potential for the GEB load shifting strategy. Especially, pre-cooling and pre-heating are considered effective for load shifting. Using the thermal inertia of buildings is a cost-effective way to reduce peak load without sacrificing comfort [20]. Turner et al. [21] investigated mechanical pre-cooling in low thermal mass homes to shift peak electricity loads using the simulation tool across various climates. Their approach balanced energy efficiency and occupant comfort by optimizing pre-cooling strategies and thermostat settings. Reinforcement learning methods [22–24] have been studied for the control of HVACs at the building level. In these studies, reinforcement learning has been used to achieve load shifting and comfort assurance in multiple HVAC systems. The implementation of smart grid technologies and the Internet of Things plays a crucial role in improving load shifting capabilities in GEBs. Finn et al. [25] discovered that household dishwashers, when subjected to a control algorithm aimed at minimizing cost and carbon emissions, exhibited peak load shifting at time between 28% and 70%. Farzamkia et al. [26] reported that the maximum load of the refrigerator can be shifted by about 11% by pre-cooling strategies and by over 40% with optimized algorithms. Glavan et al. [27] have shown that pre-cooling can result in a peak load shift of 18% for commercial refrigeration in supermarkets.

Generation

Generation is the ability to produce electricity for consumption on-site or to dispatch electricity to the grid in response to a signal from the grid operator. The GEB generation strategy is crucial to effectively integrate large-scale renewable energy and manage power flow, thereby ensuring grid stability and efficient energy use. In this generation strategy, it is assumed that power can be generated on demand for either personal or distribution purposes. However, in reality, power generation from sources like PV cannot be managed this way; hence, the use of batteries and similar technologies is a prerequisite.

Store: Electricity battery storage is a significantly flexible resource. It provides the ability to increase charging during periods of high generation and increase discharge during periods of high demand. The battery-to-demand control method is an essential technical solution for effective energy management, especially when combined with renewable energy generation on site. Several studies have investigated the utilization of battery storage to enhance the self-consumption rate of solar PV systems [28–32] and wind turbines [33]. Salpakari et al. [32] have achieved situations where over 50% of energy consumption was met by renewable generation on site, leading to negligible operational expenses. The energy storage capacity of EVs can be utilized to absorb excess energy during off-peak times and release it during peak times, aiding in load shedding and overall grid stability. This concept is explored in various smart grid frameworks, emphasizing the role of EVs and energy trading in modernizing the grid infrastructure [34, 35]. Thus, many previous studies on the GEB's generation strategy have focused on how to use up generated power in buildings. In order to utilize generated power, there is another way such as selling electricity to the grid as reverse power flow. Unahalekhaka et al. [36] explored the optimal sizing and positioning of a battery energy storage system (BESS) to minimize reverse power flow in PV system power plants. Their study concluded that installing BESS directly at the PV power plant was the most effective strategy for reducing generated energy loss, power fluctuations, and enhancing electricity production. Fokui et al. [37] proposed an intelligent control system for EV charging during peak solar production periods to mitigate reverse power flow by excess power. However, large-capacity batteries entail high costs, and discussions regarding whether their contributions justify these costs have not been conducted.

1.2.2 Flexibility Manegement of GEBs

Conventional GEBs are based on contributing to the electricity grid through load shifting and load balancing. In recent years, these shifts in demand can be created as electrical flexibility to improve the supply-demand balance and can be bought and sold with the market. As with system-level applications, operational phase applications at the building level involve evaluations of energy flexibility potential, comparisons of control strategies, and assessments of energy management strategies. Depending on whether optimization is integrated into the process, these applications can be heuristic or optimal in nature.

Interact: Regarding the heuristic method, Ramos et al. [38] conducted experiments to assess several operational techniques for HVAC systems, including modifications to set-point temperatures, preconditioning durations, and the duration of night ventilation. They simulated costs in each method under fixed, critical peak pricing, real-time pricing, and time-of-use pricing models. Pinamonti et al. [39] introduced a rule-based control approach to adjust air-source heat pumps according to the availability of PV energy. The goal is to increase the amount of PV energy consumed on-site and decrease dependence on the electrical grid. Regarding the optimization method, Good et al. [40] proposed a two-stage stochastic programming model that enables heating energy flexibility by utilizing thermal energy storage. The program determined the most efficient temperature schedules to save energy expenses while maintaining thermal comfort. Bandera et al. [41] investigated the possibility of increasing on-site PV self-consumption by exploiting the thermal mass storage of the building. The researchers utilized a genetic algorithm (GA) to optimize the schedule for the room temperature setpoint. The goal was to maximize the consumption of solar energy while maintaining thermal comfort. Conversely, when establishing coordination capacity for GEB, it is crucial to assess the potential rewards achievable through this flexibility. Hence, a critical challenge for the future lies in distinguishing buildings based on their ability to secure coordination rewards compared to others. Some research [42, 43] dissected the problem of aggregator in the management of DER and pre-bid concerns. These research conducted on bidding challenges focused on optimizing pre-bidding methods by utilizing forecasted prices obtained from market price signals. However, discrepancies between predicted prices and actual transaction prices have led to losses for aggregators and consumers, emphasizing the need for more accurate methods.

1.3 Research Questions and Approaches

This section describes the remaining research questions to maximize the potential of GEB energy management for smart energy systems. Figure 1.5 shows the scope of this dissertation, where we consider both the consumption level, the generation level, and the market level. GEBs need a system that can contribute more to the power grid without compromising on the building's objectives (electrical cost and comfort) to meet future changes in the power supply and demand environment. This dissertation addresses three questions regarding three key points of GEBs.

Question 1: How can GEBs be used to effectively utilize surplus PV generation from the viewpoint of storage?

In the context of the GEB generation strategy, planning for the operation of DERs, particularly PV generation, is imperative. This planning serves as a critical tool to evaluate the performance of GEBs and estimate long-term electrical costs. Renewable energy production, especially PV generation, exhibits substantial fluctuations with seasonal variations due to changes in temperature and solar radiation. This variability introduces the risk of generating surplus power that cannot be controlled and must be managed. As discussed in Section 1.2, research on these issues, mainly in relation to battery linkages, is underway because the battery can temporally shift the generated power. Therefore, methods that only consider the use of power within the building can lead to situations where generated electricity is wasted, depending on the capacity of the generation sys-

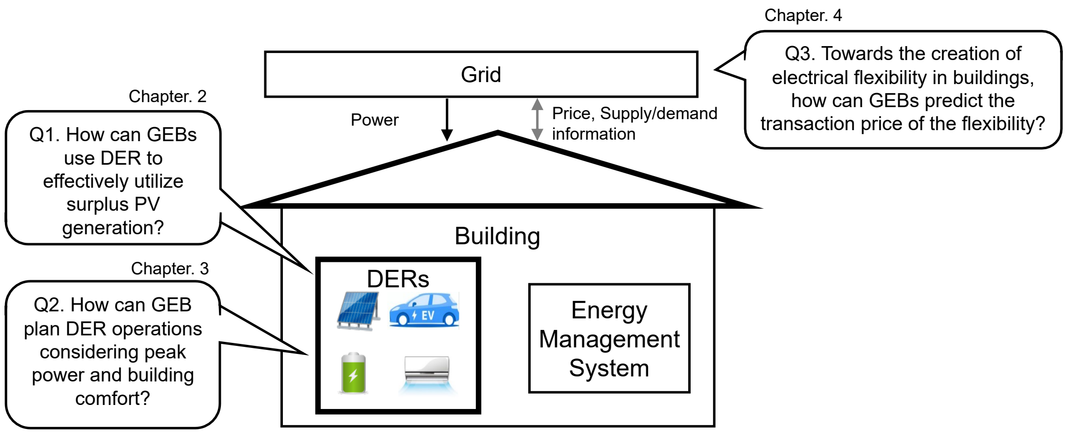

Figure 1.5: Study scope of this dissertation

tem. Another solution is to sell surplus power back to the grid, providing an opportunity to utilize wasted renewable energy elsewhere and fill spatial gaps within the energy framework. However, large-scale reverse power flow often compromises grid stability, highlighting the need for effective solar energy use without such reverse power flow. Recent studies have explored planned reverse power flow to minimize its impact on the grid. However, within the context of GEBs, as the integration of large-scale renewable energy progresses, there is a growing need for new generation strategies beyond traditional reverse power flow and battery utilization.

Using EV charging and discharging is a potential way to utilize surplus PV generation. EVs are gaining popularity due to their low carbon footprint, and the widespread installation of charging stations further supports their adoption. Typically equipped with high-capacity batteries for extended ranges, these batteries are often not fully utilized in daily operations. This underutilization presents an opportunity to bridge the temporal and spatial gap between energy supply and demand. Numerous studies explore the integration of solar energy and EVs, focusing on load shedding and profit maximization. However, there is a gap in research that focuses on minimizing solar energy waste. Therefore, a method is needed that not only enhances efficiency through temporal power shifting via EVs but also spatially and temporally shifts surplus power, leveraging the mobility of EVs. This approach maximizes the utilization of PV power generation without relying on reverse power flow, thereby minimizing waste. The proposed approach contributes at least partly to the generation strategy.

Question 2: How can GEBs effectively schedule DER operations considering peak power and building comfort from the viewpoint of consumption?

In GEBs, the realization of load shedding and shifting is increasingly being sought through DERs, especially HVAC systems. HVAC is crucial due to its high demand within buildings and existing installations, reducing additional costs. Various studies have been conducted on the realization of load shedding and shifting through HVAC systems, as introduced in Section 1.2. The main methods used for this are model predictive control (MPC) and reinforcement learning for HVAC scheduling. However, each method has advantages and disadvantages. MPC uses indoor environmental forecasts for long-term scheduling, its computation time increases with more units. On the other hand, reinforcement learning faces challenges like the need for extensive data and uncertainty about comfort. Therefore, there is a demand for methods that realize load shedding and shifting in GEBs while controlling the increase in computation time and guaranteeing comfort.

This dissertation investigates HVAC management in GEBs for effective load shedding and shifting, focusing on user comfort and cost minimization under power grid constraints using the MPC method. The proposed methodology divides HVAC operations optimization into two parts: power resource allocation to each HVAC system and operational scheduling. First, power allocation determines each HVAC's upper power limitation based on HVAC ability and user. Next, the operational scheduling problem is formulated as a multi-objective optimization, balancing electricity costs and thermal comfort, and incorporating the power limits from the initial allocation. The proposed method offers a solution to meet power constraints in multiple units. Traditional approaches to optimizing multiple HVAC units as a single problem led to increased computation time. Therefore, this research is a key aspect of the energy management framework for GEBs.

Question 3: How can GEBs predict the transaction price of electrical flexibility for efficient interaction with the market?

The evolving role of GEBs in the electricity supply and demand balancing market has shifted from basic power consumers to a more dynamic participation, enhancing adaptability in energy systems. GEBs are now instrumental in the efficient integration of renewable energy sources, such as solar and wind power, into the grid, optimizing their use without waste. This integration is crucial, especially when managing variable energy sources and mitigating grid overloads during peak demand.

Moreover, for GEBs participating in the supply and demand balancing market, accurately predicting market transaction prices is essential. These predictions are key to formulating effective strategies, allowing GEBs to buy or sell energy optimally, maximizing revenue, and establishing efficient energy supply approaches. Accurate market forecasts also give GEBs a competitive advantage, enabling them to offer more efficient and competitive energy services. Therefore, focusing on strategies for precise market price predictions is vital for GEBs to effectively and strategically participate in the supply and demand balancing market. This forecasting is a significant step towards a sustainable energy system.

1.4 Organization

The rest of this dissertation is organized as follows. Chapter 2 presents a framework that causes charging and charging of EVs, as energy trading, through an EV aggregator intentionally changing price. This framework aims to reduce solar energy waste through energy trading. The results of the experiment demonstrate that the proposed framework effectively reduced solar energy waste by 68%.

Chapter 3 presents a method for scheduling multiple HVAC systems. The proposed technique allocates electrical power to each HVAC system based on its occupancy and outdoor unit. Subsequently, the scheduling of each HVAC system is designed to ensure that the overall power consumption remains below the power limits imposed by peak demand. The results of the experiment demonstrate that the proposed approach successfully generates a schedule that conforms to the power limitation at all times without compromising thermal comfort.

In Chapter 4, a market price forecasting model is introduced for the frequency control ancillary services (FCAS) market. The model examines forecasting models derived from a wholesale market and considers markets with different response times as input data, including the target market operated by the australian energy market operator (AEMO). The proposed forecasting model achieves an RMSE of 7.8$/MWh on the energy price in the 6-Second-Raise market of AEMO, as observed by the experiments. The proposed forecasting model significantly decreases the root mean square error (RMSE) by 80% compared to the forecast price released by AEMO.

Chapter 5 serves as the concluding section of this dissertation, providing a summary of the main points discussed and suggesting potential areas for further research.

Chapter 2

Spatiotemporal Energy Shifting via EV Aggregator

Solar energy is a widely adopted energy source these days, playing a vital role in achieving a sustainable society. Within the broader scope of grid-interactive efficient buildings (GEBs) and distributed energy resources (DERs) management, particularly photovoltaic (PV) generation, strategic planning is crucial to evaluate GEB performance and estimate long-term electrical costs. While GEBs typically export surplus solar energy as reverse power flow, this extensive reverse flow can often lead to instability in the power grid. For effective utilization of renewable energy and reduction of solar energy waste, electric vehicles (EVs) play a crucial role in bridging the spatiotemporal gap in solar energy distribution. This chapter presents a new EV aggregation framework designed to facilitate the spatiotemporal redistribution of solar energy without reverse power flow. The proposed framework causes charging and charging of EVs, as energy trading, through an EV aggregator intentionally changing price. This framework aims to reduce solar energy waste through energy trading. Simulation results indicate that the proposed framework successfully reduced solar energy waste by 68%.

2.1 Introduction

The use of solar energy is increasingly recognized as key to achieving a sustainable society and is being adopted widely these days. The international renewable energy agency reports that there has been impressive growth in solar energy capacities, which have increased by 1046 GW from 2006 to 2022 [4]. In GEBs, PV generation stands as a key DER. Effective utilization of solar energy often encounters issues due to temporal and spatial mismatches between energy demand and supply. Solar panels, for example, only generate power during the day, which causes a temporal gap as this energy is not readily available at night. Additionally, the spatial gap presents a challenge, as renewable energy sources are frequently distributed across various locations. Batteries play a crucial role in bridging the temporal gap in the utilization of solar energy, often installed alongside PV panels in homes. They enable the use of renewable energy even at night, effectively addressing the temporal gap. Regarding the grid-interactive efficient buildings (GEB) generation strategy, planning the operation of distributed energy resources (DERs), especially PV generation, is essential. This planning is key for evaluating GEB performance and estimating long-term electrical costs. When solar power cannot be used or stored at home, the excess is often sold back to the grid, utilizing otherwise wasted energy elsewhere and addressing the spatial gap. However, extensive reverse power flow can lead to grid instability, highlighting the need for alternative methods to use solar energy without reverse flow.

With the rise in popularity of EVs due to their low carbon emissions, charging stations are now widely accessible. These EVs typically feature large batteries for extended range, but in daily use, these batteries often remain underutilized. This implies that the EV battery has the potential to overcome temporal and spatial gaps in energy demand and supply. Numerous studies have been conducted on the connection between solar energy and EVs [44–55]. Cui et al. introduced an optimization framework for scheduling EV batteries to assist in peak load shaving [48]. This approach allows EVs to both charge and discharge on-site. Although this research focuses primarily on peak shaving and profit maximization, it notably lacks a focus on minimizing solar energy waste.

This chapter introduces a new EV aggregation framework designed to minimize solar energy waste. The framework, drawing inspiration from Cui's model, allows EVs to both charge and discharge on-site, purchasing excess energy from households with abundant energy. This approach effectively reduces solar energy waste without necessitating a reverse power flow. A unique pricing strategy underpins this system, setting different prices for energy-rich and energy-poor households to facilitate the redistribution of excess energy.

The contributions in this chapter are summarized as follows.

- This research introduces a new framework for managing EV aggregation, aimed at minimizing the waste of solar energy. This framework has led to a significant reduction in solar energy waste, achieving a decrease of up to 68%, and, at the same time, the purchased energy from the grid was also reduced by 13%.
- This research explores the impact of battery sizes in households and EVs on the effectiveness of the proposed EV aggregator.

The structure of the remaining chapter is outlined as follows: Section 2.2 delves into relevant literature and studies. Section 2.3 describes the system model, while Section 2.4 details the proposed methodology. Section 2.5 presents the experimental results, and the chapter concludes with Section 2.6, summarizing the findings and implications.

Table 2.1: Summary of research on EV aggregators

Ref.	Year	Object	Approach
[44]	2010	Peak shaving	Charge/discharge scheduling
[45]	2010	Peak shaving	Charge scheduling
[46]	2015	Maximizing profits	Dynamic pricing
[47]	2017	Maximizing profits	Dynamic pricing
[48]	2017	Peak shaving	Charge/discharge scheduling
[49]	2018	Load reduction	Dynamic pricing
[50]	2018	Peak shaving	Charge/discharge scheduling
[51]	2018	Peak shaving	Charge scheduling
[52]	2018	Peak shaving	Dynamic pricing
[53]	2020	Maximizing profits	Dynamic pricing
[54]	2020	Maximizing profits & Peak shaving	Dynamic pricing
[55]	2021	Maximizing profits	Dynamic pricing

2.2 Related Research

2.2.1 Researches on EV Aggregators

The rising popularity of EVs has significantly increased their charging demand, posing a risk to grid stability. EV aggregation emerges as a potential solution to this issue. Table 2.1 provides an overview of research in EV aggregation. Initially focusing on peak demand shaving since its first study in 2010, the field has evolved to include profit maximization, with studies exploring various models like EV, grid, price, and traffic. Current EV aggregation strategies primarily use dynamic pricing, enabling indirect control of EV charging and discharging behaviors after initially dominating scheduling-based methods.

Some research has proposed the EV aggregation method for the peak shaving [44, 45, 48, 50–52]. Sadeghianpourhamami et al. [50] analyzed the usage patterns of the charging stations of EVs, and this knowledge optimizes the charging / discharge schedule. This research investigated the potential to mitigate peak electricity demand by managing EV charging schedules, leveraging the insights gathered from these data. Chen et al. [51] developed and tested models for EV charging schedule patterns in various scenarios of energy consumption. This research analyzed the effects of EV charging behavior on global load characteristics and demonstrated that appropriate charging patterns can reduce peak electricity demand.

Several studies propose the pricing mechanism fpr the EV aggregator to maximize the profitability of electricity transactions [46, 47, 53–55]. Moghaddam et al. [54] introduced a pricing control technique that uses reinforcement learning. This research achieved the objectives of reducing peak electricity demand and maximizing profits for

EV aggregators. However, this research did not include considerations for reducing solar energy waste. The objective of this chapter is to transfer excess solar energy between households using an EV aggregator to charge and discharge EVs. To the best of author's knowledge, this research is the first to address the reduction of solar energy waste by EV aggregation.

2.2.2 Researches on Energy Management

In this part, research related to energy management at the consumer level is introduced, which is necessary as a prerequisite for aggregation. Energy management methods on the consumer side, including households and business buildings, etc., have been investigated to optimize the utilization of solar energy. In [56–59], the main objective of these researches includes reducing the total demand and cutting the peak demand by scheduling the household battery and smart appliances. Watari et al. [57] introduced an energy management approach that considers battery management. This research successfully implemented effective battery management techniques and minimized the electricity bill. The research, cited in [57], provides complementary research because this chapter focuses on EV and EV aggregator. In this chapter, the household model is supposed to include both the household appliances and the EV, and an EV aggregation framework is proposed to connect the EV aggregator with the EVs that are associated with these household models. The household model operates under the assumption that energy management is optimized to provide maximum benefit, and the behavior of EVs is determined based on this model.

2.3 System Model

This section presents the system model for the proposed EV aggregation framework. It envisions a scenario where traditional charging stations are replaced by an EV aggregator that can charge and discharge EVs. Figure 2.1 illustrates this system model of the proposed framework. The model includes I household models, each with an EV, and one EV aggregator model. The chapter aims to reduce solar energy waste through spatiotemporal shifting via EVs, facilitated by interactions between the household and EV aggregator models.

2.3.1 Household Model

As depicted in Figure 2.1, each household is equipped with a PV panel, electric load, battery, power router, and an EV. Residents utilize their EVs for commuting between their homes and the EV aggregator. When an EV is connected to the house, the EV functions as an additional fixed battery. The power router, receiving pricing information from the EV aggregator, enables the EV to engage in energy transactions through

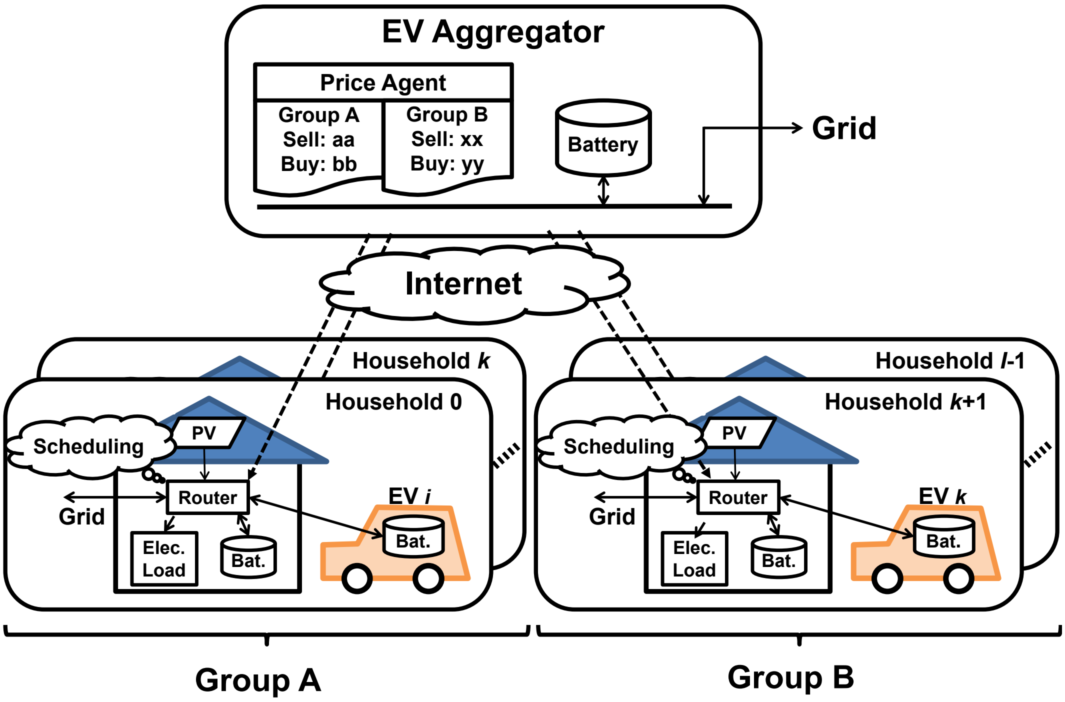

Figure 2.1: System model: household model and EV aggregator model

discharging or charging at the EV aggregator. The power router determines battery scheduling to minimize electricity bills and maximize profit. For example, during peak hours when the grid has excess generation in the daytime, it is not recommended to sell electricity generated by the household as reverse power flow due to its detrimental effect on the grid. During off-peak hours, households can send their surplus solar energy to the grid as reverse power flow. If the batteries are fully charged and there is PV power that cannot be consumed, the surplus solar energy is wasted or can be sold back to the grid as reverse power flow. The power router transmits the EV battery schedule (the schedule for charging or discharging the EV in the EV aggregator) and the energy budget to the EV aggregator at regular intervals. In addition, the power router obtains the current price data from the EV aggregator and carries out the iterative scheduling process using the updated information. The household model and the EV aggregator model perform these interactions in an iterative manner.

2.3.2 EV Aggregator Model

The EV aggregator is expected to function as both a large parking facility and a charging station. Figure 2.2 shows the physical structure of the EV aggregator. A physical structure is assumed to consist of a parking lot with a large battery connected to it. The EV aggregator is equipped with both charging and discharging capabilities, along with

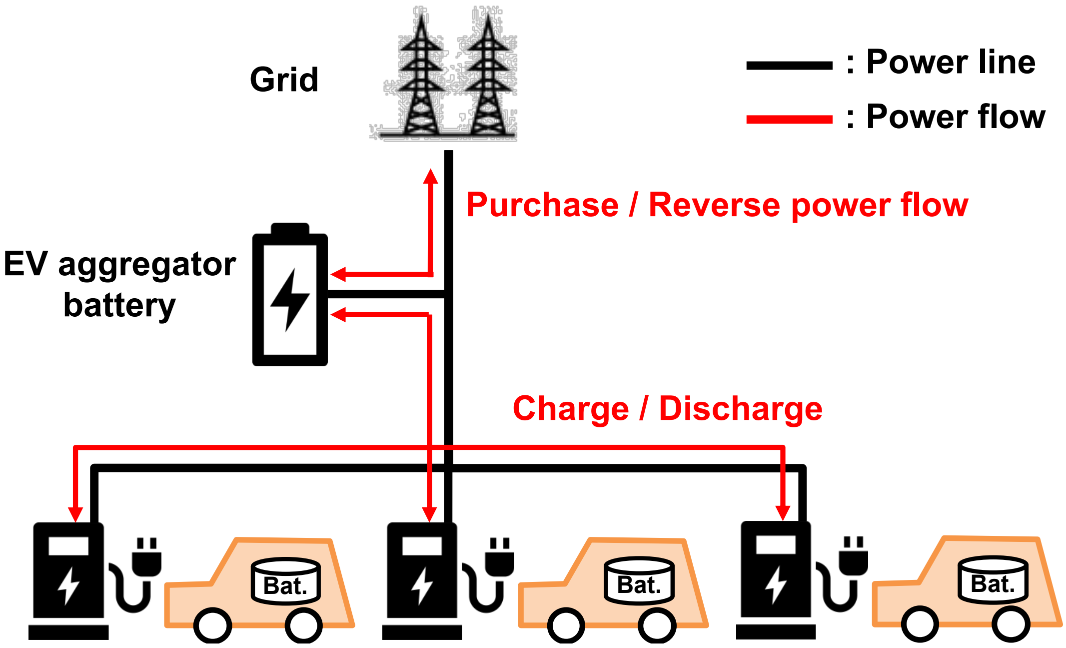

Figure 2.2: Overview of power flow in EV aggregator

a substantial fixed battery. In this system, batteries and charging/discharging facilities are interconnected at the grid connection point. The setup includes a sufficient number of these facilities, ensuring that EVs can connect for charging or discharging upon arrival. In proposed EV aggregator, multiple EVs can charge and discharge electricity at the same time. Additionally, the EV aggregator includes a price agent responsible for setting energy trade prices with the EVs. The EV aggregator pre-receives the battery schedule and energy budget from households. The fixed battery of the EV aggregator handles all energy requests for EV charging/discharging. When the EV aggregator cannot meet the charging demand of EVs due to insufficient battery capacity, it compensates by purchasing energy from the grid. Alternatively, if the EV's discharged energy cannot be stored in the EV aggregator's battery because it is fully charged, the surplus energy is then sold to the grid.

Electricity trading assumes that the EV aggregator sets a higher price for selling electricity than the price at which it buys from EVs. Based on this assumption, energy-rich households are incentivized to sell their surplus energy to the EV aggregator instead of wasting it within households. On the other hand, energy-poor households are incentivized to purchase electricity from EV aggregators, as the selling prices offered by aggregator are lower than those of the grid. Through such electricity trading, the EV aggregator can make a profit. However, the primary objective of EV aggregators is not profit maximization but rather the extent to which wasted energy can be shifted. Hence, the EV aggregator sets prices based on its objectives. The EV aggregator classifies EVs

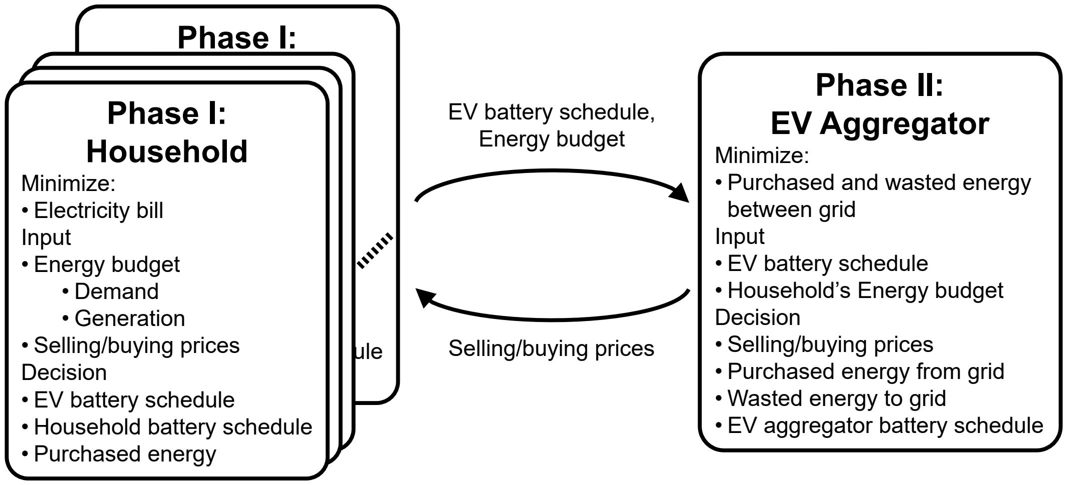

Figure 2.3: Overview of the spatiotemporal energy shifting method

into two categories based on their energy budget. This classification aims to collect surplus energy from the energy-rich and redistribute it to the energy-poor. The energy budget information is sent from each household. Research on forecasting the next day's demand [60, 61] and generation [62, 63] at each household has advanced sufficiently, and it is assumed that these data are available. If households have wasted energy, they are classified into the energy-rich group (Group A). If households do not have wasted energy, they are classified into the energy-poor group (Group B). The pricing agent of the EV aggregator establishes distinct prices for each group, then communicates the respective prices to the household model. The pricing agent adjusts these prices based on the remaining battery capacity of the EV aggregtor and the energy budget of each household. The updated prices are transmitted to households through the internet.

2.4 Problem Formulation

This section introduces a method for the spatiotemporal shifting of solar energy waste. The aim is to reduce solar energy waste by redistributing it between households and the EV aggregator, using EVs as a carrier. The focus of this chapter is on the interaction between the household and the EV aggregator, which is crucial for the effective implementation of this method. Figure 2.3 shows an overview of the proposed method. The method proposed in the research is structured into two phases. Phase I involves scheduling the household battery to minimize electricity bills. Phase II encompasses battery scheduling and updating prices at the EV aggregator. These phases are executed iteratively to induce a spatiotemporal shift in wasted energy. The study adopts an online algorithmic approach, allowing households to adjust their behaviors flexibly at each control interval. This flexibility is based on their current energy situation and the

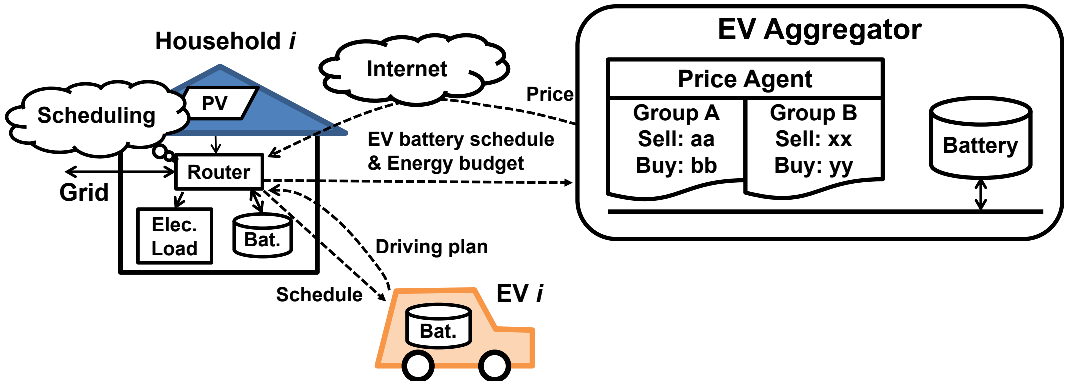

Figure 2.4: Phase I: Scheduling to minimize the electricity bill of the household

pricing from the EV aggregator. As a result, the EV aggregator's prices and household behaviors are fine-tuned through iterative calculations, eventually reaching a natural convergence.

In Phase I, each household plans their battery usage and the amount of energy they purchase, with the objective of minimizing their electricity bill. The inputs for this phase include the selling and buying prices at the EV aggregator, as well as forecasted data on PV generation and electricity demand. Every household transmits their EV battery schedule and energy budget to the EV aggregator.

In Phase II, the EV aggregator collects all household information. This information outlines the requests for charging and discharging the EVs and the energy budget for each household. In response to the information received, the EV aggregator arranges its own battery usage, energy purchases from the grid, and the management of excess energy. Following this, the EV aggregator revises the selling and buying prices. The EV aggregator sets two distinct prices for groups categorized as energy-rich and energy-poor, based on their future energy budgets. It then communicates the relevant price to each household according to their classification. Following the introduction of the updated prices, the EV battery schedules are then adjusted to align with these updated prices. The next subsections describe the details of each phase.

2.4.1 Phase I: Household Battery Scheduling for Electricity Bill Minimization

Figure 2.4 shows an overview of Phase I. In Phase I, households schedule their battery usage to minimize their electricity bills. Each household's problem is expressed using mixed integer programming (MIP), with the planning period. The planning period is defined as $0 \leq u < U$, u is a time step, and U is the overall period. The problem formulation is derived from prior research [64].

Let $Bh_u^{IN}, Bh_u^{OUT}, Bv_u^{IN}, Bv_u^{OUT}, S_u, B_u, Q_u, Y_u, Z_u$ be the amount of energy used to charge or discharge the battery of the household, the amount of energy used to charge or discharge the EV battery connected to the household, the amount of energy selling or buying in the EV aggregator, the reverse power flow energy, the amount of wasted energy and the amount of energy purchased at time u, respectively. These variables are the decision variables.

Denote BS^h as the size of the household battery, and $\overline{SOC^h}$ and $\underline{SOC^h}$ as the upper and lower limits of the state of charge (SOC) level, respectively. The remaining energy of the household battery Xh_u should meet the following formulation at every time u.

$$\underline{SOC^h} \leq \frac{Xh_u}{BS^h} \leq \overline{SOC^h} \qquad 0 \leq u < U \tag{2.1}$$

Additionally, the remaining energy Xh_u can be updated by the following equation.

$$Xh_{u+1} = Xh_u + Bh_u^{IN} - Bh_u^{OUT} \qquad 0 \leq u < U-1 \tag{2.2}$$

The remaining energy in the EV's battery Xv_u is represented in the same way. Denote BS^v as the size of the EV battery, and $\overline{SOC^v}$ and $\underline{SOC^v}$ as the upper and lower limits of the SOC level, respectively. The remaining energy Xv_u should meet the following formula at every time u.

$$\underline{SOC^v} \leq \frac{Xv_u}{BS^v} \leq \overline{SOC^v} \qquad 0 \leq u < U \tag{2.3}$$

The method of updating the remaining energy of the EV varies depending on the situation of the EV. The state of EVs is denoted by the variable ds_u. ds_u can take values of zero, one, and two, representing being connected to a household, disconnected, and connected to an EV aggregator, respectively. The remaining energy of the EV, denoted as Xv_u, can be updated using the following equation.

$$Xv_{u+1} = \begin{cases} Xv_u + Bv_u^{IN} - Bv_u^{OUT} & \text{if } ds_u = 0 \\ Xv_u - H & \text{if } ds_u = 1 \\ Xv_u - S_u + B_u & \text{if } ds_u = 2 \end{cases}$$
$$0 \leq u < U-1 \tag{2.4}$$

It should be noted that the energy used for driving at each time step can be simplified and represented by a constant value, denoted as H. Charging and discharging of the EV's battery are permitted only when $ds_u = 0$, and when the EV is connected to the household. This implies that Bv_u^{IN} and Bv_u^{OUT} are zero when ds_u is equal to one or two, indicating that the EV is not linked to the household. Similarly, if $ds_u = 2$ and the EV is linked to the EV aggregator, it is permitted to buy and sell energy in the EV aggregator. Therefore, if ds_u is equal to zero or one and the EV is not linked to the EV aggregator, both S_u and B_u remain zero.

Denote G_u as the PV generation and D_u as the electricity demand at time u. The power flow inside the household needs to conform to the following constraint.

$$\begin{aligned} &Z_u + G_u + Bh_u^{OUT} + Bv_u^{OUT} \\ &\quad - (Q_u + Y_u + D_u + Bh_u^{IN} + Bv_u^{IN}) = 0 \qquad 0 \leq u < U \end{aligned} \tag{2.5}$$

The constraint equations related to surplus solar energy are defined as follows.

$$Q_u = 0 \qquad \text{if on-peak} \tag{2.6}$$

$$Y_u = 0 \qquad \text{otherwise} \tag{2.7}$$

During periods when the electricity system produces more power than needed during the daytime, households are not allowed to send surplus power to the grid as reverse power flow to maintain grid stability. Hence, surplus solar energy is disposed of as wasted energy. Reverse power flow can occur during off-peak hours, eliminating wasted energy.

The objective of this problem is to minimize the electricity bill. The objective function can be expressed as follows, using price information: R_u, Ps_u, and Pb_u. R_u, Ps_u, and Pb_u denote the grid electricity price, the selling prices at the EV aggregator at time u, and the buying prices at the EV aggregator at time u, respectively.

$$\begin{aligned} &\text{minimize :} \\ &\qquad \sum_{u=0}^{U-1} \{R_u \cdot Z_u - (Ps_u \cdot S_u - Pb_u \cdot B_u)\} \end{aligned} \tag{2.8}$$

The objective function does not account for the reverse power flow. Typically, Japanese electric power companies (such as Kansai Electric Power Company, Inc.) only permit the reverse power flow for energy generated by PV systems. Hence, the objective function of this model excludes reverse power flow to avoid the occurrence of reverse power flow from batteries. This model assumes the implementation of time-of-use (TOU) pricing. TOU pricing provides two distinct pricing structures: peak pricing and off-peak pricing. The definition of R_u is as follows.

$$R_u = \begin{cases} R_{high} & \text{if peak-time} \\ R_{low} & \text{otherwise} \end{cases} \tag{2.9}$$

R_{high} and R_{low} represent the peak price and off-peak price, respectively.

As previously stated, the household model transmits the schedule of EV batteries and energy budget, denoted S_u, B_u, G_u, and D_u, to the EV aggregator at set time intervals.

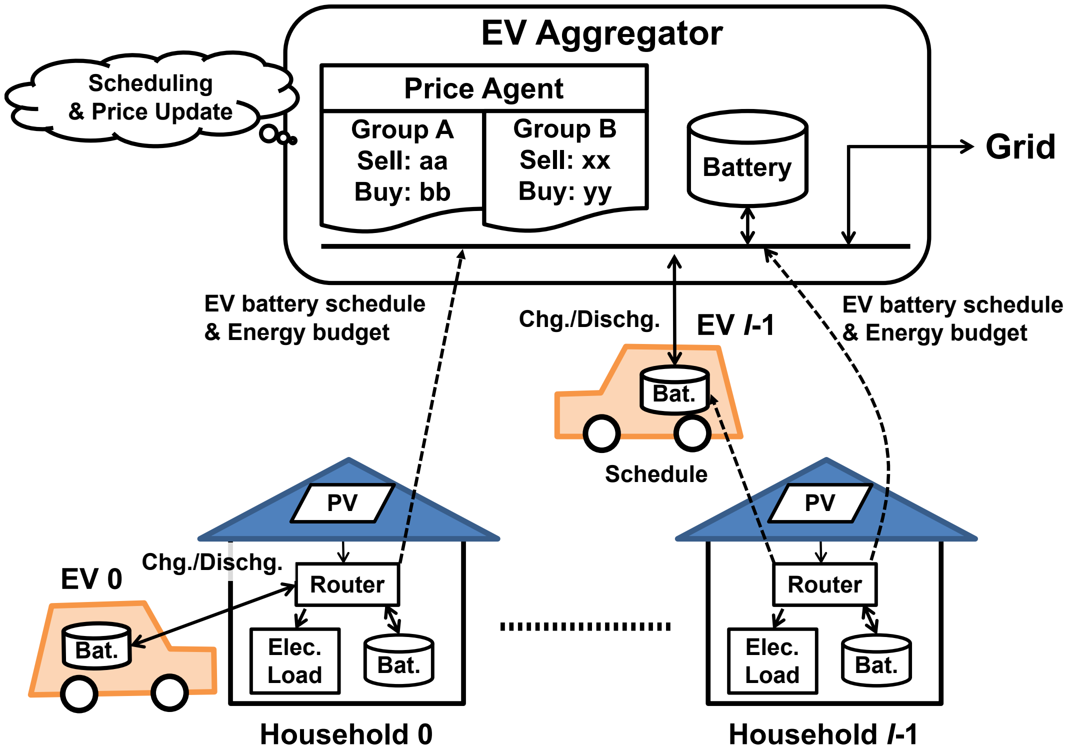

Figure 2.5: Phase II: Scheduling of aggregator battery and price update based on the battery sufficiency

2.4.2 Phase II: Battery Scheduling and Price Update at EV Aggregator

Figure 2.5 provides an overview of Phase II. In Phase II, the EV aggregator collects all information from the households, indicating the charge / discharge request and the energy budget. Responding to household requests, the EV aggregator optimizes its battery schedule and updates the prices for selling and buying energy based on the remaining battery energy. The EV aggregator differentiates between two groups: Group A (energy-rich) and Group B (energy-poor), classified according to their energy budget. Each group is offered a specific price, which is then communicated to households. This leads to an update of the EV battery schedule in each household. This research aims to indirectly supply the energy-poor with energy waste from the energy-rich through these iterations of EVs and EV aggregator.

Battery Scheduling

The battery scheduling of the EV aggregator is formulated in this section using MIP. The EV aggregator determines its own battery schedule from all given EV battery schedules in order to minimize the total energy purchased and the amount of reverse power flow.

The EV aggregator determines its own battery plan based on all EV battery schedules to minimize the total energy purchased and the amount of reverse power flow. The planning period is $0 \leq u < U$. The EV aggregator obtained the EV battery schedule and the energy budget from EV i, where the range of i is defined as $0 \leq i < I$. The variables S_u, B_u, G_u, and D_u associated with EV i are redenoted as $S_{i,u}$, $B_{i,u}$, $G_{i,u}$, and $D_{i,u}$ in this section, respectively.

Denote V_u as the amount of purchased energy from the grid, and W_u as the amount of reverse power flow to the grid by the EV aggregator at time u. V_u and W_u are decision variables.

Define BS^{st} as the battery size of the EV aggregator, $\overline{SOC^{st}}$ as the upper bound of the SOC level, and $\underline{SOC^{st}}$ as the lower bound of the SOC level. The remaining energy of the EV aggregator's battery, denoted Xs_u, must adhere to the following equation for every time u.

$$\underline{SOC^{st}} \leq \frac{Xs_u}{BS^{st}} \leq \overline{SOC^{st}} \qquad 0 \leq u < U \tag{2.10}$$

The remaining energy change of the EV aggregator's battery Xs_u can be defined using the following equation.

$$Xs_{u+1} = Xs_u + V_u - W_u + \sum_{i=0}^{I-1}(S_{i,u} - B_{i,u}) \qquad 0 \leq u < U-1 \tag{2.11}$$

The objective function of EV aggregator is defined as follows.

$$\text{minimize}: \quad \sum_{u=0}^{U-1} V_u + \sum_{u=0}^{U-1} W_u \tag{2.12}$$

In order to address this issue, the EV aggregator determines its own battery schedule based on given all the battery schedules of the EVs.

Price Update

In order to minimize wasted energy by shifting energy from the energy-rich to the energy-poor using EVs and EV aggregator, the EV aggregator categorizes incoming EVs into two categories based on their energy budget: Group A – energy-rich group and Group B – energy-poor group. The EV aggregator differentiates between group A and group B based on the daily household's generation and demand balance at each control period. Households that produce a greater amount of energy are categorized as Group A. In contrast, households with a higher demand are categorized as Group B.

Define EV_A as the set of EVs in Group A and EV_B as the set of EVs in Group B. EV_A and EV_B are defined as follows.

$$EV_A = \left\{ i \in I \middle| \sum_{u=0}^{U-1} D_{i,u} \leq \sum_{u=0}^{U-1} G_{i,u} \right\} \tag{2.13}$$

$$EV_B = \left\{ i \in I \middle| \sum_{u=0}^{U-1} D_{i,u} > \sum_{u=0}^{U-1} G_{i,u} \right\} \tag{2.14}$$

The EV aggregator sets two prices for EV_A and EV_B, and this section explains the method of updating these prices.

During on-peak hours, households in this research dispose of surplus solar energy as wasted energy. To prevent the wastage of solar energy in households, EV aggregators purchase energy from households through EVs. Denote Pb_u^A as the buying price offered to households in Group A, and Pb_u^B as the buying price offered to households in Group B. Pb_u^A and Pb_u^B are as follows.

$$Pb_u^A = PB \qquad 0 \leq u < U \tag{2.15}$$

$$Pb_u^B = PB \qquad 0 \leq u < U \tag{2.16}$$

where PB means the constant price to buy the wasted energy.

As stated in Section 2.4.1, this research utilizes time-of-use (TOU) pricing, which includes two types of prices: R_{low} and R_{high}. An EV aggregator aims to spatiotemporally redistribute solar energy waste, with a primary focus on shifting such energy to the energy-poor. Furthermore, the EV aggregator sets the price of selling electricity higher than the price of buying EVs to avoid losing money. Thus, the EV aggregator sets the constant buying price PB and three constant selling prices PS_{low}, PS_{middle}, and PS_{high} to keep the following relation.

$$PB \leq PS_{low} < R_{low} \leq PS_{middle} < R_{high} \leq PS_{high} \tag{2.17}$$

PS_{low}, PS_{middle} and PS_{high} are selected for for EV_A and EV_B.

Let Ps_u^A, Ps_u^B be the selling prices to the households in Group A and Group B, respectively. Ps_u^A and Ps_u^B are selected as follows.

$$Ps_u^A = PS_{high} \qquad 0 \leq u < U \tag{2.18}$$

$$Ps_u^B = \begin{cases} PS_{high} & \text{if } \frac{Xs_u}{BS^{st}} < SOC_{LB}^{st} \\ PS_{middle} & \text{if } SOC_{LB}^{st} \leq \frac{Xs_u}{BS^{st}} < SOC_{UB}^{st} \\ PS_{low} & \text{otherwise} \end{cases} \qquad 0 \leq u < U, \tag{2.19}$$

where SOC_{LB}^{st} and SOC_{UB}^{st} represent the lower border and upper border of the SOC level. The pricing policy aims to primarily transfer the accumulated solar energy waste to households in EV_B. Consequently, households in EV_A is always charged the highest selling price PS_{high}. The EV aggregator collects surplus energy from Group A and shifts it to Group B.

2.5 Experiments

This section details simulation experiments that validate the effectiveness of the proposed framework. The experimental setup is initially described, followed by case studies conducted under various scenarios. In Section 2.5.1, the effectiveness of the proposed framework in reducing solar energy waste is demonstrated. The discussion in Section 2.5.2 focuses on the trade-off between the size of the battery and the impact of the EV aggregator.

The experiment includes a total of 100 households, denoted by the variable I in the framework. The planning period for the optimization issue is 24 hours, divided into intervals of 30 minutes each, denoted by $U = 48$. The simulation period lasts 90 days, and the suggested approach is executed once every 30 minutes throughout the simulation duration. The optimization issue is defined and solved using the IBM ILOG CPLEX Optimization Studio v.12.7 mathematical programming solver [65]. The remaining parameter configurations are shown in Table 2.2. The designated on-peak hours, during which reverse power flow is not allowed, were established to be 7 am to 11 pm, aligning with the peak-time period of the time-of-use (TOU) price. The TOU price of the grid differentiates between daytime and nighttime prices; hence, this setting is followed in the analysis. The parameters BS^h and BS^v are individually selected from Table 2.2. The initial SOC of the household battery, the EV battery, and the EV aggregator battery is set to 0.5. EVs are utilized randomly between the hours of 9:00 and 22:00, with an average duration of 5 hours. This time duration covers both driving and parking. The power demand and power generation data used as household profiles

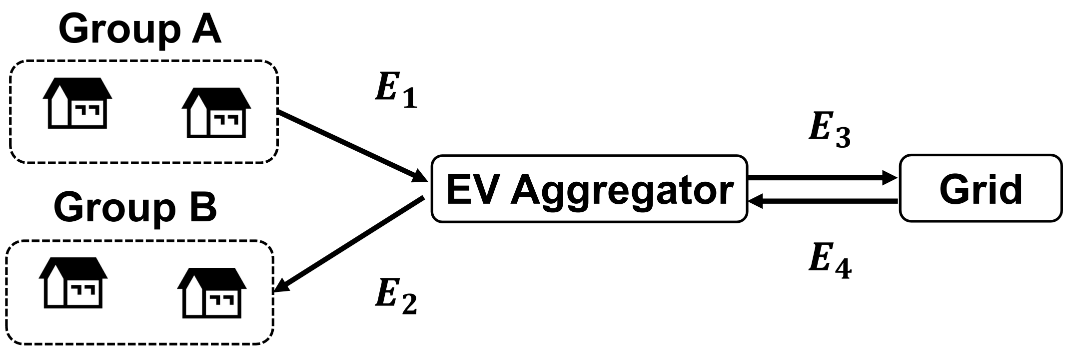

Figure 2.6: Overview of energy shifting

Table 2.2: Parameter setting

Parameter	Value	Unit
BS^h	$5, 10, 15$	kWh
$\overline{SOC^h}$	1.0	-
$\underline{SOC^h}$	0.1	-
BS^v	$40, 60, 80, 100$	kWh
$\overline{SOC^v}$	1.0	-
$\underline{SOC^v}$	0.1	-
on-peak	$7:00-23:00$	-
peak-time	$7:00-23:00$	-
R_{high}	21.27	JPY/kWh
R_{low}	10.51	JPY/kWh
BS^{st}	1000	kWh
$\overline{SOC^{st}}$	1.0	-
$\underline{SOC^{st}}$	0.1	-
PB	5	JPY/kWh
PS_{low}	8	JPY/kWh
PS_{middle}	16	JPY/kWh
PS_{high}	21.27	JPY/kWh
SOC^{st}_{LB}	0.5	-
SOC^{st}_{UB}	0.75	-

are measured in New South Wales, Australia [66].

The experiment aims to verify the effectiveness of the proposed method for the utilization of wasted energy. To assess this, a comparative simulation is conducted: one scenario implements the proposed method with an EV aggregator, and the other uses only charging stations without an EV aggregator.

2.5.1 Effectiveness in Reducing Wasted Energy

This section assesses the efficacy of the proposed framework in reducing the waste of solar energy. Nine scenarios are considered, each with varying frequency of EV utilization and number of Group A and Group B. These scenarios are presented in Table 2.3. These scenarios imply that an EV is utilized twice or four times each week, or every weekday and randomly on weekends. As an illustration, Scenario 5 shows that every household uses an EV aggregator on a frequency of four occasions per week, with 50

Table 2.3: Scenarios

	EV utilization frequency			Number of households in Group A / Group B
	Twice a week	Four times a week	Every weekday +Random weekends	
Scenario 1	×			30 / 70
Scenario 2		×		30 / 70
Scenario 3			×	30 / 70
Scenario 4	×			50 / 50
Scenario 5		×		50 / 50
Scenario 6			×	50 / 50
Scenario 7	×			70 / 30
Scenario 8		×		70 / 30
Scenario 9			×	70 / 30

Table 2.4: Summary of output

Output	Description
E_1	Amount of energy shifted from Group A to EV aggregator
E_2	Amount of energy shifted from EV aggregator to Group B
E_3	Amount of energy shifted from EV aggregator to grid
E_4	Amount of energy shifted from grid to EV aggregator

out of 100 households belonging to Group A. The differentiation between Group A and Group B in the experimental scenarios is determined by the overall balance of electricity demand and generation for 90 days, as indicated by Equations (2.13) and (2.14). BS^h and BS^v are set to 10 kWh and 40 kWh, respectively.

First, some metrics are introduced to evaluate the performance of the proposed framework. Figure 2.6 illustrates the transfer of energy between the EV aggregator, households, and the power grid, while Table 2.4 offers a comprehensive description of the output. The percentage reduction in wasted energy α_{wasted} and the percentage reduction in purchased energy $\alpha_{purchase}$ are given by Equations (2.20) and (2.21). Y_i and Y_i' denote the sum of wasted energy by the household i in scenarios with and without an EV aggregator, respectively. Z_i and Z_i' denote the sum of purchased energy only from the grid by the household i, in scenarios with and without an EV aggregator, respectively. Consequently, Z_i excludes the energy purchased from the EV aggregator.

$$\alpha_{wasted} = \frac{\sum_{i=0}^{I-1} Y_i' - \sum_{i=0}^{I-1} Y_i}{\sum_{i=0}^{I-1} Y_i'} \cdot 100 \tag{2.20}$$

$$\alpha_{purchase} = \frac{\sum_{i=0}^{I-1} Z_i' - \sum_{i=0}^{I-1} Z_i}{\sum_{i=0}^{I-1} Z_i'} \cdot 100 \tag{2.21}$$

Table 2.5: Power trading result and profit of EV aggregator

	E_1 (kWh)	E_2 (kWh)	E_3 (kWh)	E_4 (kWh)	EV aggregator's profit (JPY)
Scenario 1	5,651	5,664	0	0	64,449
Scenario 2	4,568	4,715	0	0	71,908
Scenario 3	2,328	2,419	0	0	40,165
Scenario 4	10,018	10,036	0	0	80,278
Scenario 5	8,486	8,682	0	0	124,861
Scenario 6	4,821	4,942	0	0	81,017
Scenario 7	15,622	15,582	0	0	69,311
Scenario 8	14,303	14,445	0	0	169,590
Scenario 9	8,778	8,894	0	0	143,843

Table 2.6: Purchased energy and wasted energy of households

	Purchased energy (kWh)		Wasted energy (kWh)		$\alpha_{purchase}$ (%)	α_{wasted} (%)
	with EVA	without EVA	with EVA	without EVA		
Scenario 1	103,349	108,130	3,060	7,398	4	59
Scenario 2	121,458	125,185	1,943	5,191	3	63
Scenario 3	141,520	143,394	2,214	3,881	1	43
Scenario 4	85,072	93,566	5,719	13,558	9	58
Scenario 5	101,739	108,923	3,203	9,654	7	67
Scenario 6	121,748	125,857	3,540	7,224	3	51
Scenario 7	61,137	74,603	9,940	22,575	18	56
Scenario 8	75,400	87,655	5,080	16,438	14	69
Scenario 9	95,038	102,754	5,210	12,259	8	57

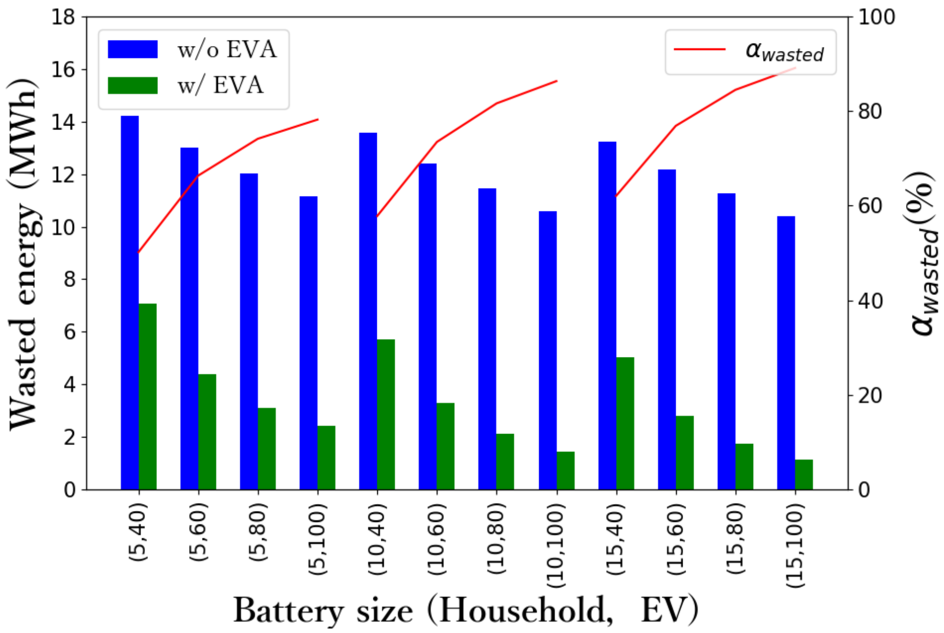

Figure 2.7: Wasted energy for each combination of battery size in Scenario 4

The experimental results for each scenario are shown in Table 2.5 and 2.6. The results shown in Table 2.5 show that households participate in electricity trading within the EV aggregator and that the EV aggregator consistently generates profit in all scenarios. The result of E_1 indicates that energy is shifted from Group A to EV aggregators. The result of E_2 shows that the energy is shifted from EV aggregators to Group B. In all scenarios, the value of E_1 is nearly identical to the value of E_2. Regarding the pricing of the EV aggregator, after the EV aggregator collects electricity from Group A, the EV aggregator offers Group B a price that is lower than the price of the grid. As a result, Group B buys almost all of the energy that Group A sells to the EV aggregator. In addition, the EV aggregator refrained from selling the energy acquired from Group A to the grid. This is due to the EV aggregator's aim to minimize its energy buying and selling with the grid, as defined in its objectives. Therefore, E1 and E2 are almost the same amounts. The analysis of results for E_3 and E_4 in Table 2.5 indicates that the EV aggregator did not sell power to the grid or buy energy from it. Table 2.5 reveals that the EV aggregator makes profits in all scenarios, despite the objective function of the proposed method that does not specifically aim to maximize profits. These findings indicate that the shift of energy through the EV aggregator was effectively achieved without the need to buy or sell energy from or to the grid.

The results in Table 2.6 show the total purchased energy and wasted energy for households in each scenario with and without the EV aggregator, respectively. Addition-

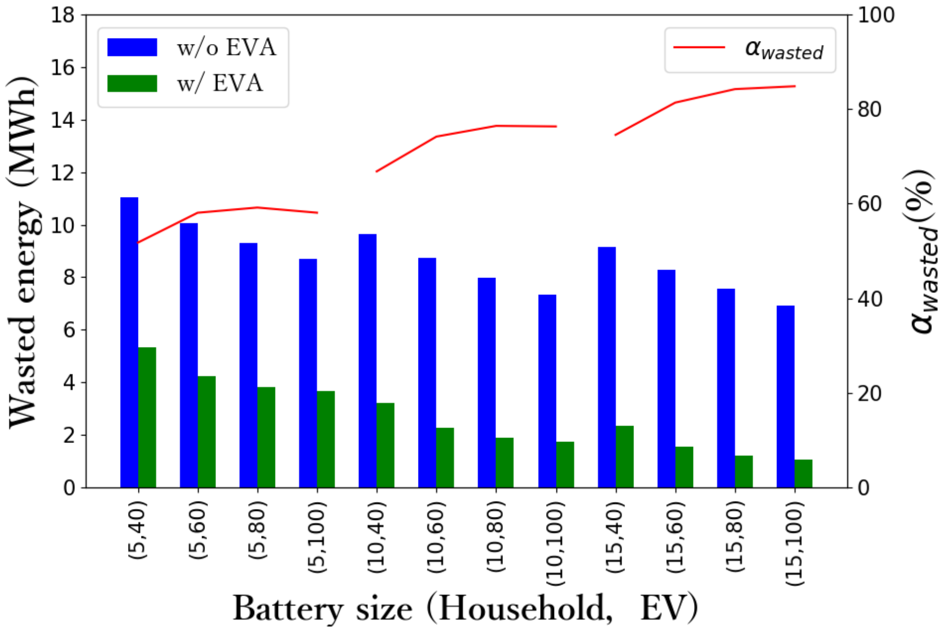

Figure 2.8: Wasted energy for each combination of battery size in Scenario 5

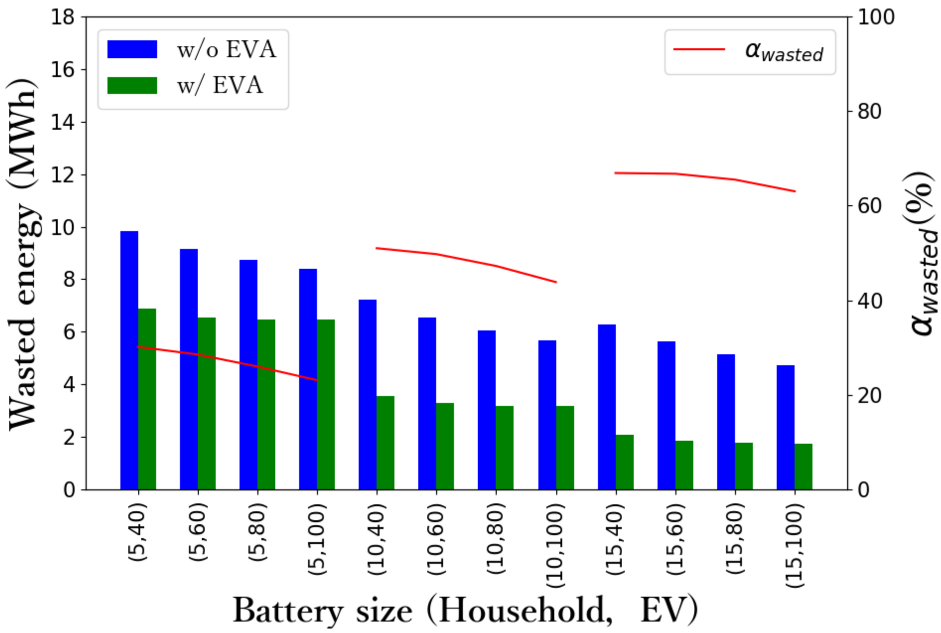

Figure 2.9: Wasted energy for each combination of battery size in Scenario 6

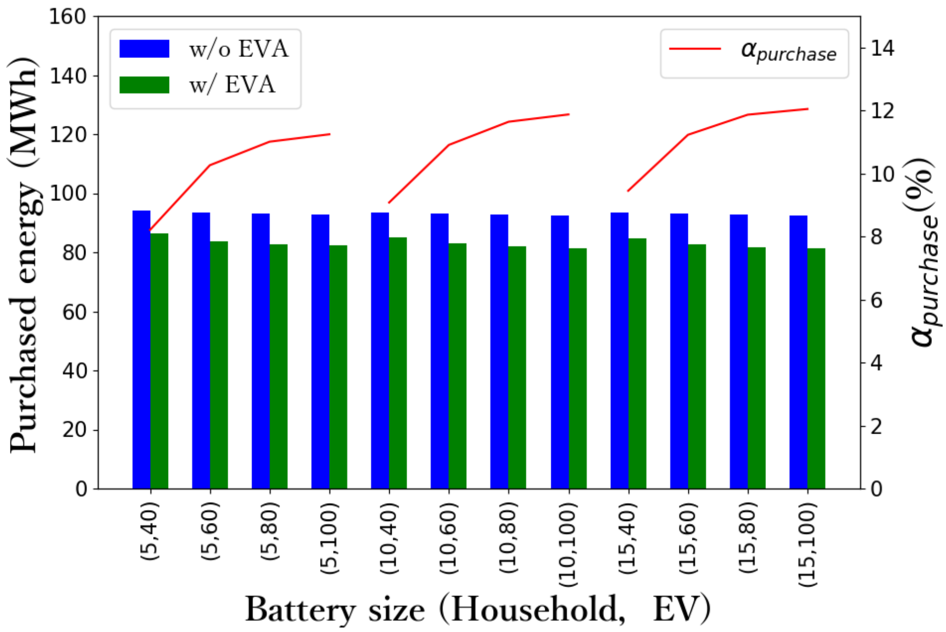

Figure 2.10: Purchased energy for each combination of battery size in Scenario 4

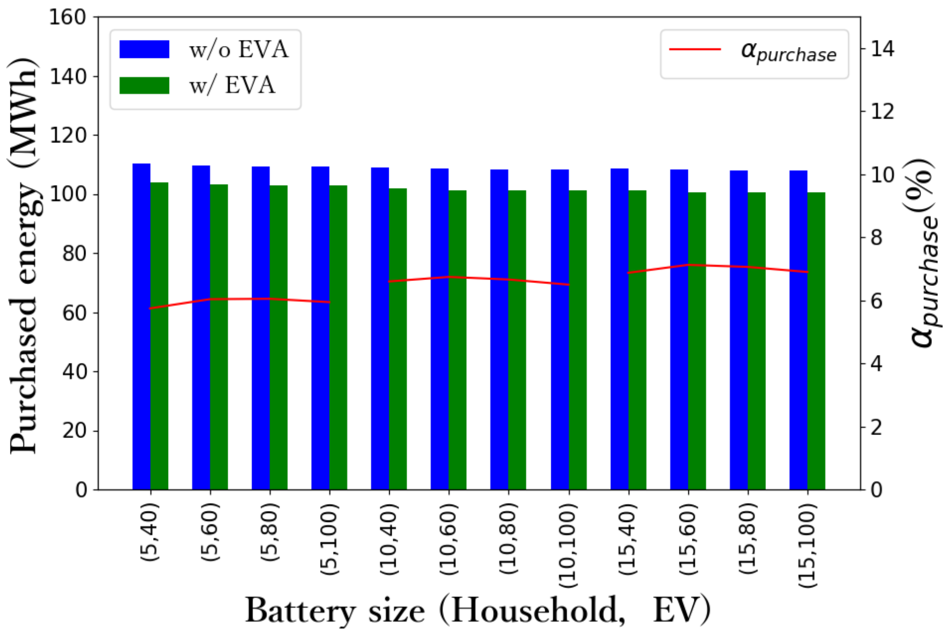

Figure 2.11: Purchased energy for each combination of battery size in Scenario 5

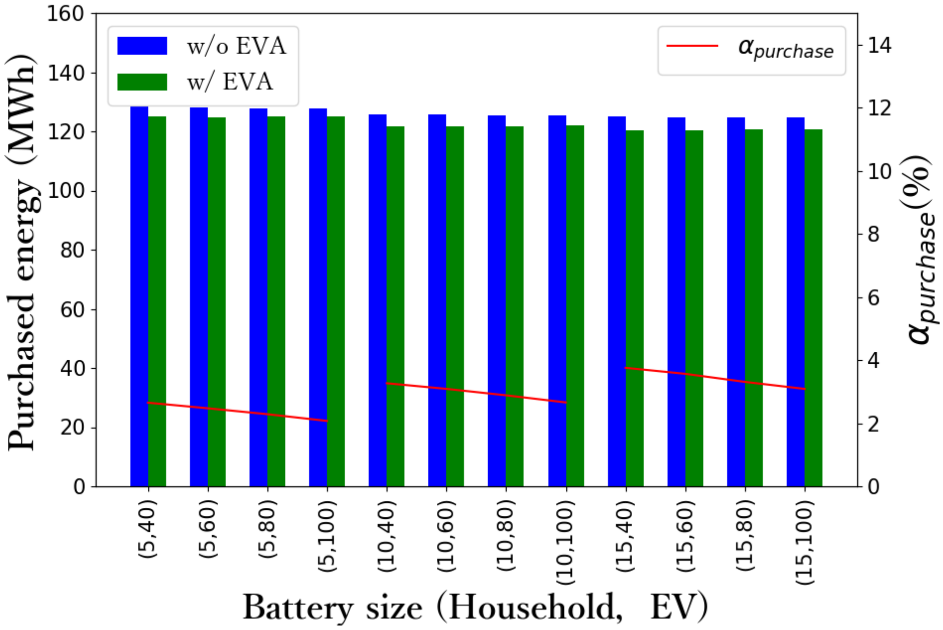

Figure 2.12: Purchased energy for each combination of battery size in Scenario 6

ally, Table 2.6 shows the reduction rates of purchased energy ($\alpha_{purchase}$) and wasted energy (α_{wasted}) achieved through the proposed method. As shown in Table 2.6, $\alpha_{purchase}$ and α_{wasted} are positive. The proposed method consistently reduces both the purchased energy and wasted energy of households in all scenarios. The primary aim of this chapter is to shift surplus energy; therefore, the effectiveness of the proposed method is best demonstrated by the reduction in wasted energy α_{wasted}. The reduction in this wasted energy is at least 43%. On the other hand, $\alpha_{purchase}$ tends to be low in all scenarios. However, the proposed method successfully achieves spatial energy shifting, previously possible only through the grid, by using EV batteries. It has succeeded in reducing purchased energy without relying on the grid. Therefore, the proposed EV aggregator successfully reduces purchased energy and wasted energy.

Table 2.6 indicates a difference between the total reduction in purchased energy and the total reduction in wasted energy. This difference is due to the varying amount of battery charge at the end of each experiment.In this experiment, no specific conditions were set for the amount of battery charge at the end of the simulation. This variation resulted in differences in the total reduction in purchased energy and the total reduction in wasted energy by the proposed method.

The results from Scenario 8 indicate that the proposed method can achieve a maximum reduction of wasted energy by 68%, without reverse power flow. In the same scenario, the proposed method also enabled a shift of wasted energy to Group B, resulting in a 13% reduction in the energy they purchased from the grid. Compared to Scenario 1 and Scenario 7, $\alpha_{purchase}$ increases, while α_{wasted} remains nearly unchanged when the number of households in Group A increases. A higher value of $\alpha_{purchase}$ implies a decrease in the amount of purchased energy from the grid by households. When comparing Scenarios 1 and 7, it is observed that Scenario 7 has a higher number of households that are energy-rich. The increasing number of households with higher PV generation results in an increase in the total amount of wasted energy. Therefore, the proposed method becomes more effective in shifting a larger amount of energy from Group A to Group B through the EV aggregator. Consequently, there was a decrease in the amount of purchased energy in Group B, which led to a reduction in $\alpha_{purchase}$. In Scenario 7, while the total amount of wasted energy is increasing, there is also a corresponding increase in the energy shift from Group A to the EV aggregator (E1). Therefore, the percentage reduction of wasted energy remained the same and there is almost no change in α_{wasted}. The results of all scenarios demonstrate the effectiveness of the proposed method for shifting solar energy waste. This shifting occurs between Group A (energy-rich) and Group B (energy-poor) through the EV aggregator and is achieved without reverse power flow.

2.5.2 Impact of Battery Size on Proposed Method

This section examines the influence of battery size on the proposed technique, taking into account various sizes of EV batteries and household batteries. The experiment employs Scenarios 4, 5, and 6 as described in Table 2.3. All combinations of BS^h and BS^v for these scenarios are evaluated.

Figures 2.7, 2.8, and 2.9 illustrate the amount of energy wasted in Scenarios 4, 5, and 6, both with and without the EV aggregator. The x-axis represents the various combinations of battery sizes. The left y-axis represents the amount of energy that is wasted, while the right y-axis provides the percentage reduction of wasted energy, denoted as α_{wasted}. The red line represents the value of α_{wasted}, while the blue and green bars represent the amount of wasted energy in scenarios without an EV aggregator and with an EV aggregator, respectively.

In each scenario, the introduction of the EV aggregator consistently reduces wasted energy. The extent of this reduction varies depending on the battery size combination and the specific scenario. In Scenario 4, with infrequent EV usage, the EV aggregator and larger battery size significantly influence the outcome. Conversely, in Scenario 6, where EVs are used more frequently, the aggregator's impact is less pronounced due to less energy waste compared to other scenarios.

Figures 2.10, Figure 2.11, and Figure 2.12 illustrate the amount of energy purchased in Scenarios 4, 5, and 6, both with and without an EV aggregator, respectively. The x-axis represents the various combinations of battery sizes. The left y-axis represents the amount of energy purchased, while the right y-axis indicates the percentage reduction of the purchased energy, denoted as $\alpha_{purchased}$. The red line represents the value of $\alpha_{purchased}$, while the blue and green bars represent the amount of purchased energy in scenarios without an EV aggregator and with an EV aggregator, respectively.

Regardless of the scenario, the proposed EV aggregator marginally decreases the amount of purchased energy. The percentage reduction in purchased energy is observed to be relatively small because the amount of purchased energy is much larger than that of wasted energy. The energy savings achieved by the EV aggregator are beneficial, especially for energy-poor households. This implies that these households may not need to purchase additional energy because of the aggregator's efficiency in reducing energy waste. Therefore, it is evident that the decrease in wasted energy resulting from the EV aggregator is equivalent to the amount of reducing purchased energy. In Scenario 6, depicted in Figure 2.12, there is a drop in $\alpha_{purchase}$ as the size of the EV battery grows, unlike in Scenarios 4 and 5. In Scenario 6, EVs are frequently used, and the amount of energy transferred through an EV aggregator is lower due to reduced energy waste compared to other scenarios. The decline in $\alpha_{purchase}$ is due to a reduction in shifted energy.

The experimental results demonstrate that the proposed method is effective in reducing and redistributing wasted solar energy. This effectiveness is consistent across different battery sizes, highlighting the method's versatility.

2.6 Summary

This chapter introduces a new EV aggregation framework designed for the spatiotemporal shifting of solar energy, eliminating the need for reverse power flow to the grid. The framework operates on the interaction between household and EV aggregator models to shift solar energy waste. Additionally, it incorporates a pricing strategy at the EV aggregator to facilitate the redistribution of wasted energy. The results of the experiment demonstrate that the proposed method effectively reduces wasted energy through the EV aggregator in all scenarios. The contribution of the proposed EV aggregator to the demand-supply balance includes the temporal and spatial shifting of surplus generated energy, which traditionally had to be discarded or reverse power flow, thereby contributing to the reduction of purchased energy for buildings. The experimental results showed a case where a reduction in purchased energy was achieved up to 14%. Regarding the contribution to GEBs, this chapter proposes a new utilization of energy by sharing it among buildings without relying on the grid, which was previously only temporally shifted within a building. Furthermore, by shifting energy through the EV aggregator, it prevents reverse power flow from buildings to the grid, enabling more grid-interactive energy management. The experiments demonstrated up to 69% effective utilization of surplus energy. Future work includes enhancing the system model by considering price elasticity on the household side during energy trading at the EV aggregator. It is necessary to take into account more comprehensive EV battery models and EV utilization models. In addition, a forecasting model is also considered for the balancing and scheduling approaches.

Chapter 3

Multiple HVAC Scheduling under Power Constraints

Significant research in grid-interactive efficient buildings (GEBs) focuses on the implementation of load shedding and shifting through various DERs, particularly heating, ventilation, and air conditioning (HVAC) systems. HVAC is crucial due to its high demand within buildings and existing installations, which reduces additional costs. This chapter discusses a scheduling method for multiple HVAC systems. The proposed scheduling technique is divided into two parts: power allocation and optimization problem. The method allocates electrical power to each HVAC system depending on the number of users and the outside unit, ensuring that the scheduling of each HVAC system is such that the overall power consumption remains under the power limit through load shedding and shifting. The results of the experiment demonstrate that the proposed method successfully acquires the schedule while adhering to the power constraint at all times without compromising thermal comfort.

3.1 Introduction

In the demand strategies of GEBs, HVAC systems play a crucial role, particularly in implementing load shedding and shifting through various DERs. Moreover, HVAC is crucial due to its high demand within buildings and existing installations, reducing additional costs. The HVAC system is a significant energy-consuming device in the residential sector, responsible for approximately 50% of its energy consumption [67]. This will clearly explain why HVAC is important to GEB's load shedding and shifting.

The studies referenced in [68] and [69] introduced mathematical programming techniques for HVAC scheduling. Through experiments conducted in real world settings, these strategies were found to maintain comfort levels and decrease electricity costs. Their attention was directed towards a single HVAC system; however, it is important to note that a building typically includes multiple HVAC systems that require regulation.

Preliminary experiments [69] revealed a problem in which attempting to simply extend the approach described in [68] resulted in too much computational complexity. Consequently, as the number of HVAC systems increased, it became impractical to address the problem in a practical time. Moreover, scheduling strategies that are specifically designed for a single HVAC system are not effective for successfully managing multiple HVAC systems simultaneously. If applied independently, a single control methodology could sometimes result in exceeding peak power limits.

The research outlines a method for scheduling multiple HVAC systems under power restriction by load shedding and shifting strategies. This proposed method involves a power allocator that assigns power to each HVAC system, taking into account the number of users and the outdoor unit capacity of each HVAC system. Within their designated power allocation, each HVAC system then carries out its own optimization process. Power allocation enables centralized management over the total power consumption of the HVAC system, independent of individual optimization. Additionally, our HVAC scheduling method is based on previous work [69]. This work takes thermal comfort into account. Therefore, the proposed method can also take comfort into account for scheduling.

The subsequent section of this chapter is structured as follows. Section 3.2 delves into the relevant literature and studies. The problem statements and the proposed technique are described in Sections 3.3 and 3.4. The results of the experiment are presented in Section 3.5, and this chapter is concluded in Section 3.6.

3.2 Related Research

Several studies have revealed the potential advantages of employing advanced control algorithms to enhance the energy efficiency of HVAC systems in both residential and commercial buildings [70–72]. The typical control strategies include proportional integral derivative (PID) [73, 74], mixed integer linear programming (MILP) [75, 76], robust optimization [77–79], stochastic programming [80, 81], and Lyapunov optimization [82, 83]. With the development of machine learning technologies, reinforcement learning (RL) [22], deep reinforcement learning (DRL) [23, 24], and MPC [84] are demonstrating their dominance in managing nonlinear systems.

On the other hand, energy management and peak control face several challenges at the building level, including GEBs. Reinforcement learning methods [22–24] are impractical for new or data-limited buildings due to their reliance on vast prior data. Yu et al. [23] developed a novel multi-agent deep reinforcement learning (MADRL) algorithm for HVAC systems in commercial buildings, significantly reducing energy costs while maintaining occupant comfort. Their approach dynamically adapts to changing occupancy and indoor conditions, demonstrating an efficient balance between energy efficiency and resident comfort. Yet, a practical challenge is the requirement for extensive HVAC usage data, a characteristic of reinforcement learning, for real-world application.

Research has also been conducted on building-level HVAC management using MPC [84, 85]. Serale et al. conducted a comprehensive study on the application of MPC for enhancing energy efficiency in buildings, particularly focusing on HVAC systems. Their approach utilized white-box, gray-box, and black-box models for precise prediction and management of building dynamics and energy use. This ensured occupant comfort through optimal thermal regulation and efficient energy strategies. One of the biggest problems with MPC for multiple HVAC management is that it is hard to find a good balance between the complexity of high-fidelity simulation models and practical computation time constraints. Therefore, an approach to building-level HVAC management that does not rely on prior data and can establish boundaries quickly within a short computation period is needed. Furthermore, the use of highly accurate room temperature change prediction models is necessary to maintain occupant comfort.

3.3 System Model

The system model for multiple HVAC systems is depicted in Figure 3.1. This model includes HVAC systems, executive servers, and a power allocator. Initially, the HVAC scheduler gathers environmental data, specifically outdoor and indoor temperatures, from both the internet and HVAC systems. Subsequently, the gathered data is used with the HVAC system model and the building thermal dynamic model. At the same time, the power allocator sends the power constraint to the executive server. The MPC determines the schedule for multiple HVAC systems at every time interval based on these data, models, and constraints. Finally, the temperature in each room is modified based on the schedule determined for each HVAC system. The scheduler optimizes the HVAC system schedule within the specified power limit to reduce the overall energy consumption while ensuring thermal comfort as long as possible. The specifics of these models are outlined in subsequent parts. The scheduling problem is formulated using mixed-integer linear programming.

3.3.1 HVAC Model

The HVAC model utilizes a coefficient of performance (COP) model to represent the thermal gain and loss of the HVAC systems. Here, COP assumes the ratio of the available heating and cooling capacity to the required energy. In this chapter, the heating and cooling capacity Q_t^{HVAC} [kW] at time step t can be calculated using the following equation:

$$Q_t^{HVAC} = COP \cdot P^{HVAC} \cdot u_t, \qquad \forall t \tag{3.1}$$

where P^{HVAC} and u_t are the rated power consumption and the load index of HVAC systems at time step t.

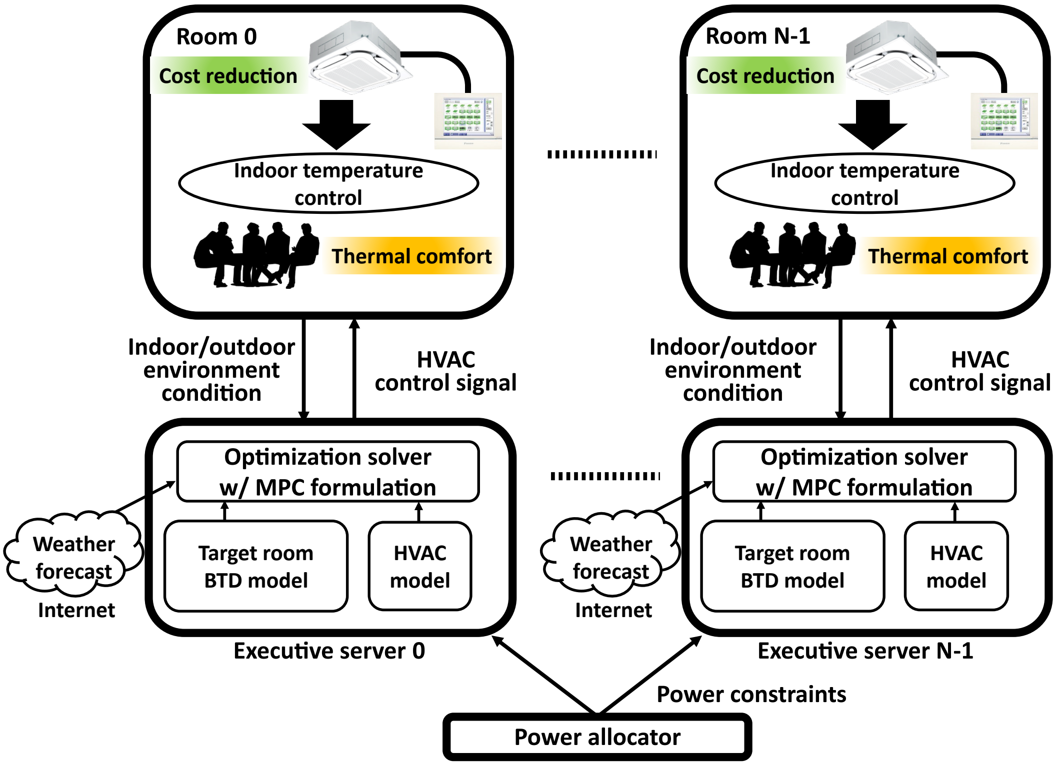

Figure 3.1: Multiple HVAC system model

3.3.2 Building Thermal Dynamic Model

The building thermal dynamic model considers the overall heat gain and loss, denoted as Q_t^{gain}, which includes the HVAC heating / cooling capacity Q_t^{HVAC} and the transfer of solar heat Q_t^{solar}, the heat generated by electronic devices Q_t^{app} and the occupants $Q_t^{personas}$, as follows:

$$Q_t^{gain} = Q_t^{HVAC} + Q_t^{solar} + Q_t^{app} + N_i \cdot Q_t^{person} \qquad \forall t \qquad (3.2)$$

$$Q_t^{solar} = I^r \cdot A_i \cdot p, \qquad \forall t \qquad (3.3)$$

where N_i, A_i, p, and I^r represent the number of users, the surface area of room i in square meters, the heat transfer coefficient between neighboring rooms, and the solar radiation intensity in kilowatts per square meter, respectively.

The thermal equivalent circuit model (TECM) is utilized for simulating the thermodynamics of buildings. The indoor temperature of the building at time t is modeled by a linear discrete-time differential equation. In the initial condition, when discrete time is used, the temperature response T^{in} of the TECM to a time step Δt is the following:

$$T_{t+1}^{in} = (1 - \Delta t/\tau_i) \cdot T_t^{in} + \Delta t/\tau_i \cdot (T_t^{out} + 1000 \cdot R_t \cdot Q_t^{gain}), \qquad \forall i, \forall t \qquad (3.4)$$

whereas T_t^{out} is the outdoor temperature. τ_i is a building time constant in secounds which can be defined as follows.

$$\tau_i = R_i \cdot C_i \qquad \forall i \tag{3.5}$$

The thermal resistance R_i and building time constant τ_i are determined based on the specifications of the building. Thermal capacitance can be determined using the relationship between R_i and τ_i as defined in Formulation 3.5.

3.4 Problem Formulation

The proposed method consists of two parts: power allocation and HVAC scheduling, which are done in power allocator and executive server of Figure 3.1, respectively. HVAC systems are assumed to provide both heating and cooling functions. The entire HVAC system is assumed to have limited power availability due to peak demand. As mentioned above, the scheduling method for a single HVAC system cannot include the total power shared between all HVAC systems. Consequently, this may lead to exceeding the peak demand. Before scheduling, the power allocator distributes the available power amoung each HVAC system. The HVAC scheduling process then performs using the power that has been allocated. The following parts describe the formulation of power allocation and HVAC scheduling.

3.4.1 Power Allocation Technique

This part presents the power allocation technique employed by the power allocator depicted in Figure 3.1. The thermal conditions within a room are influenced by the number of occupants present. Furthermore, the selection of the outdoor unit's capacity is based on the ease of changing the temperature in the room. Thus, the proposed method allocates electricity to each HVAC system based on the ratio between the number of users and the capacity of the outdoor unit. Define t as the time stamp and i as the HVAC index. The ratio $K_{i,t}^{r+c}$ is determined by considering the number of users and the capacity of the outdoor unit. To obtain the proposed ratio $K_{i,t}^{r+c}$, two power allocation ratios, namely $K_{i,t}^{res}$ and $K_{i,t}^{cap}$, are initially defined. These ratios are calculated using the number of users $c_{i,t}$ and the capacity of the outdoor unit v_n according to the following formulas.

$$K_{i,t}^{res} = \frac{c_{i,t}}{\sum_{m=0}^{N-1} c_{m,t}} \qquad \forall i, \forall t \tag{3.6}$$

$$K_{i,t}^{cap} = \frac{v_n}{\sum_{m=0}^{N-1} v_m} \qquad \forall i, \forall t \tag{3.7}$$

The allocation ratio $K_{i,t}^{r+c}$ is determined by the equation below, which is based on the allocation ratios $K_{i,t}^{res}$ and $K_{i,t}^{cap}$.

$$K_{i,t}^{r+c} = \frac{K_{i,t}^{res} \cdot K_{i,t}^{cap}}{\sum_{m=0}^{N-1} K_{m,t}^{res} \cdot K_{m,t}^{cap}} \qquad \forall i, \forall t \tag{3.8}$$

To allocate power among multiple HVAC systems, a constraint is introduced to limit the power usage of each system. S_t^{UB} represents the maximum power that can be assigned to all HVAC systems at the time t. $K_{i,t}$ represents the power allocation ratio for the HVAC system i at time t. The HVAC system i schedules its power usage within its allocated power limit, as demonstrated by the following equation.

$$D_{i,t}^{max} = S_t^{UB} \cdot K_{i,t} \qquad \forall t \tag{3.9}$$

This allocated resource $D_{i,t}^{max}$ is sent to the executive server for the room i as D_t^{max}, as shown in Figure 3.1.

3.4.2 HVAC Scheduling

The proposed method involves optimizing the HVAC system schedule separately with a power constraint using the executive server depicted in Figure 3.1. The power consumption of the HVAC system at a given time t, represented as D_t, is determined according to the thermal dynamic model of the building [86]. To do this, the energy consumption of the HVAC system D_t in each time interval is calculated as follows:

$$D_t = P^{HVAC} \cdot u_t \cdot \Delta t / 3600, \qquad \forall t \tag{3.10}$$

where P^{HVAC} represents the rated power of HVAC and u_t represents the operating rate for the rated power at time t. Then, the term of the electricity cost J_{cost} is calculated based on unit price:

$$J_{cost} = \sum_{t=0}^{M-1} \varepsilon_t \cdot D_t, \tag{3.11}$$

where M represents the total planning period.

Peak power constraints are implemented to restrict the overall energy consumption of multiple HVAC systems, as follows:

$$D_t \leq D_t^{max}, \qquad \forall t \tag{3.12}$$

where D_t is the power demand at time t, and D_t^{max} is the maximum peak power demand, which is derived from Section 3.4.1. Here, the term thermal comfort $J_{comfort}$

is calculated by taking the squared difference between room temperature T_t^{in} and the comfortable temperature T_t^{ref} as follows:

$$J_{comfort} = \sum_{t=0}^{M-1} O_t \cdot (T_t^{in} - T_t^{ref})^2, \tag{3.13}$$

where O_t is a binary variable that takes the value 1 when the room is occupied and 0 when there are no users present in the room. To mitigate the temperature limitation, a slack variable, denoted as Stc_t, is introduced as follows:

$$T_t^{lower} - Stc_t \leq T_t^{in} \leq T_t^{upper} + Stc_t, \quad \forall t \tag{3.14}$$

$$T_t^{lower} = T_t^{ref} - \Delta T, \quad \forall t \tag{3.15}$$

$$T_t^{upper} = T_t^{ref} + \Delta T, \quad \forall t \tag{3.16}$$

where ΔT represents an acceptable temperature range. The slack variable, denoted Stc_t, basically assumes zero when the room temperature is in the acceptable range. However, it becomes positive when the room temperature is beyond the bound. When the mistake in predicting the room temperature is significant and over the threshold in practical use, the optimization problem might be adjusted to prevent infeasibility.

Thus, the problem of optimizing schedule for the HVAC system can be expressed as follows:

$$\text{minimize} \quad \omega \cdot \sum_{t=0}^{M-1} J_{cost} + (1-\omega) \cdot \sum_{t=0}^{M-1} J_{Comfort} + P_e \cdot \sum_{t=0}^{M-1} Stc_t, \tag{3.17}$$

where $\omega (0 < \omega < 1)$ is the weight coefficient for balancing the trade-off between electric cost and thermal comfort. P_e represents the penalty constant associated with temperature violations. The optimization solution is obtained by considering the load index u_t in each time interval t to reduce the electric cost and enhance thermal comfort. By setting P_e sufficiently large for both J_{cost} and $J_{comfort}$, the proposed approach keeps the occupant comfortable.

3.5 Experiments

Experiments were conducted to demonstrate the efficacy of the proposed technique. It is assumed that there are four independent HVAC systems for cooling, each serving a separate room. Table 3.1 shows the distinct characteristics of each room, such as the utility time, the number of users, and the outdoor unit capacity of the HVAC systems. The HVAC systems are scheduled for a duration of 24 hours. During the scheduling process, a constraint on power consumption is imposed, allowing a maximum of 5 kW between 8:00 and 12:00. Total power consumption of HVAC systems is specifically

Table 3.1: Experimental identification of rooms

	Room 1	Room 2	Room 3	Room 4
Utility time	9-12, 13-18	7-16	9:30-15	7-11, 13-14, 15:30-17
Number of users	40	20	3	20
Outdoor unit (kW)	22.4	33.5	14.0	22.4
Rated power [kW]	5.4	8.9	3.3	5.4
C_i	14,390,109	18,314,684	7,195,054	14,390,109
R_i	0.00252981	0.0019877121	0.00505963	0.00252981

Table 3.2: Average difference between indoor and comfortable temperature during power limitation ($°C$)

	Room 1	Room 2	Room 3	Room 4
# of users only ($K_{i,t}^{res}$)	0.16	0.38	0.28	0.15
Capacity only ($K_{i,t}^{cap}$)	0.58	0.11	0.06	0.17
Both ($K_{i,t}^{r+c}$)	0.18	0.11	0.35	0.17

subject to this restriction, which must not exceed the set limit. In the experiments, ω is set to 0.1, giving greater importance to comfort in the objective function. As parameters for comfort, the comfortable room temperature T_t^{ref} is 20°C and the allowable room temperature ΔT error is 2°C. In addition, the three allocation ratios obtained from Equations (3.6), (3.7), and (3.8) are used and the results are evaluated.

Table 3.2 shows the mean difference between indoor and comfortable temperature under power limitation when various allocation ratios are used. Figures 3.2, 3.3, and 3.4 show the experimental results for the case of $K_{i,t}^{res}$ and $K_{i,t}^{cap}$ and $K_{i,t}^{r+c}$, respectively. In each figure, (a) and (b) depict the simulation results for the power consumption and indoor temperature in the four rooms, respectively.

The provided time period, from 0:00 to 19:00, is specifically excerpted to examine outcomes during the power limitation period. The yellow area denotes the time period during which available power is limited, specifically from 8:00 to 12:00. The dotted line indicates the absence of any occupants in the room. On the contrary, the solid line indicates the room being occupied by the full number of users.

Figure 3.2 demonstrates a significant peak just before the power restriction period. However, there is unused power immediately after the power restrictions are initiated. This phenomenon arises from considering only the number of occupants for power allocation and restricting power usage solely to the designated period. Consequently, pre-cooling could not be executed during the power restrictions, leading to high-power operation of HVAC units with suboptimal performance just before the restriction.

Comparing the room temperature error during the power restriction period in Rooms

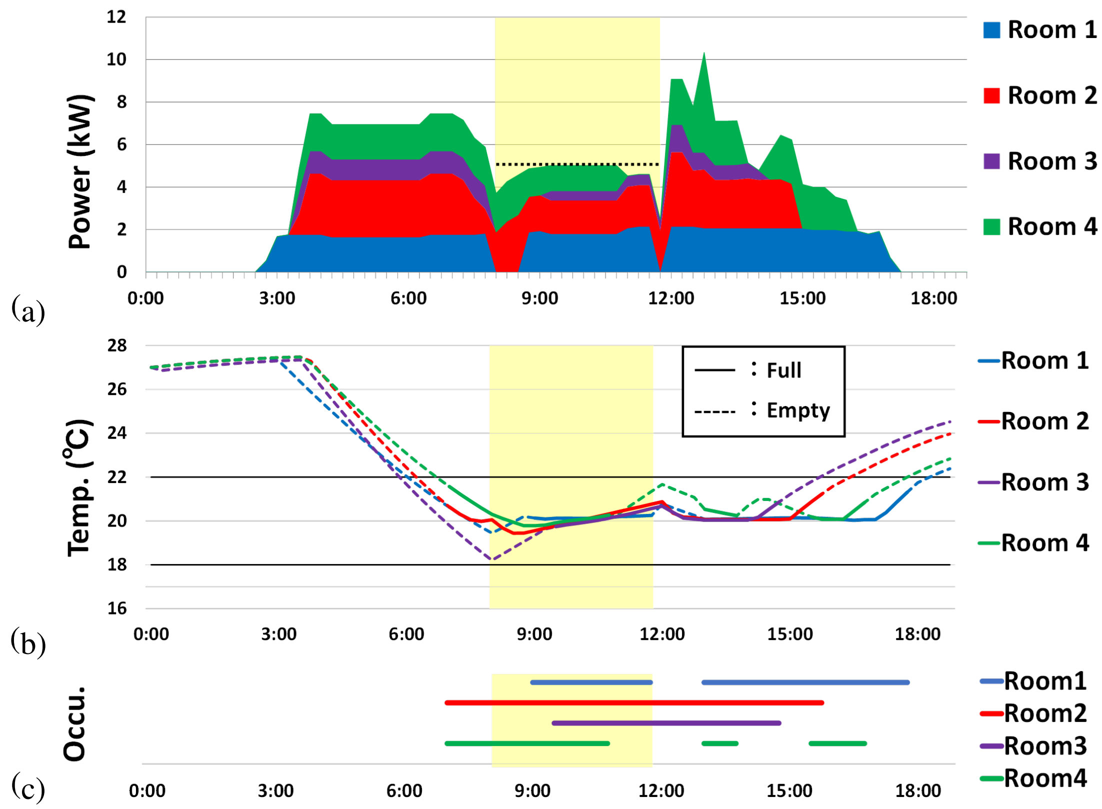

Figure 3.2: Simulation result for $K^{res}_{i,t}$: (a) power consumption and (b) indoor temperature, under (c) given occupancy schedule.

2 and 4 in Table 3.2, where the user count is similar, it's evident that the room temperature error is higher in Room 2. As shown in Figure 3.2, although Room 2 uses more energy than Room 4, Room 2 has a greater room temperature error. This discrepancy is attributed to the power resource allocation, based on user count, failing to accurately distribute power to each outdoor unit. Room 2 received insufficient cooling power due to this misallocation. Additionally, it was observed that power remained unused in several instances during the power restriction period due to the same reason.

Comparing the room temperature errors during the power restriction period in Rooms 1 and 4 in Table 3.2, both equipped with similar outdoor unit capacities, reveals that Room 1 experiences a larger room temperature error. As shown in Figure 3.3, there is no big difference in the energy consumption of rooms 1 and 4. This discrepancy stems from the power resource allocation method, which was based on outdoor unit capacity but failed to consider the specific heat load in each room. Consequently, Room 2 did not receive sufficient cooling power due to this misallocation.

Comparing the room temperature error using the two methods mentioned earlier, the proposed approach successfully achieved uniform cooling across all rooms without

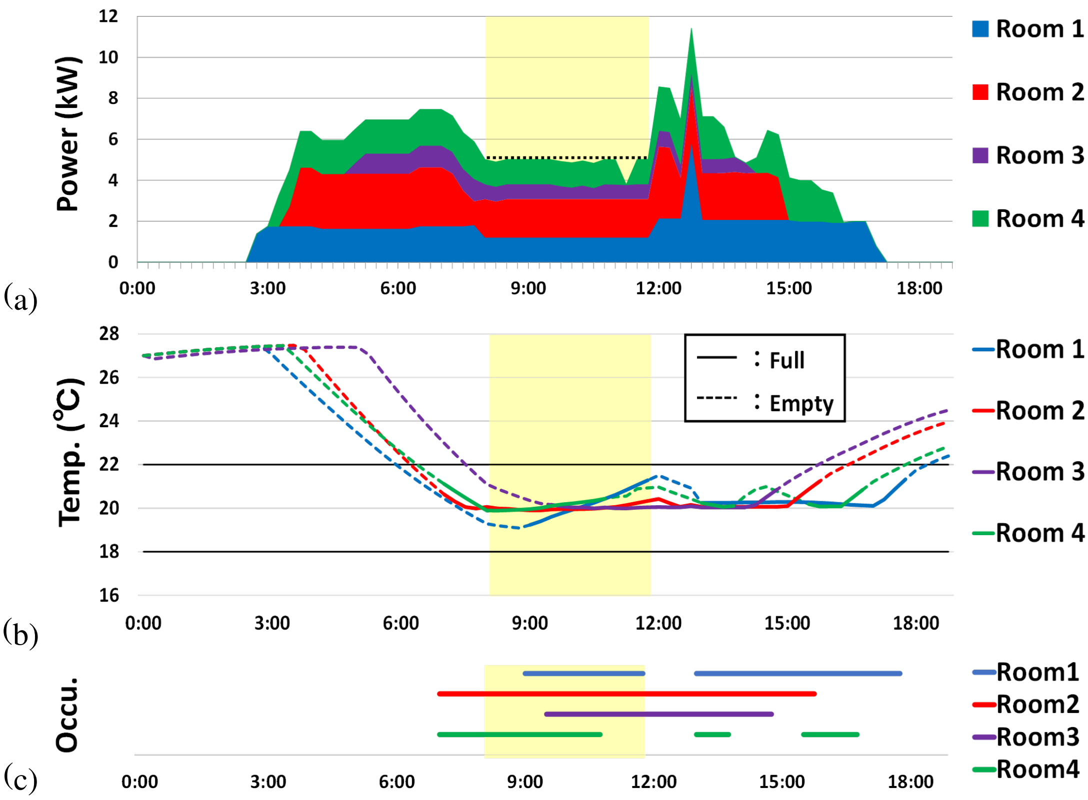

Figure 3.3: Simulation result for $K_{i,t}^{cap}$: (a) power consumption and (b) indoor temperature, under (c) given occupancy schedule.

a significant increase in total energy consumption. As shown in Figure 3.4, this result was achieved by allocating power based on both the outdoor unit specifications and the number of occupants in the room, effectively addressing the heat load within each room. The proposed technique successfully controls the HVAC systems in the rooms without exceeding the power limit or compromising the comfort of the temperature.

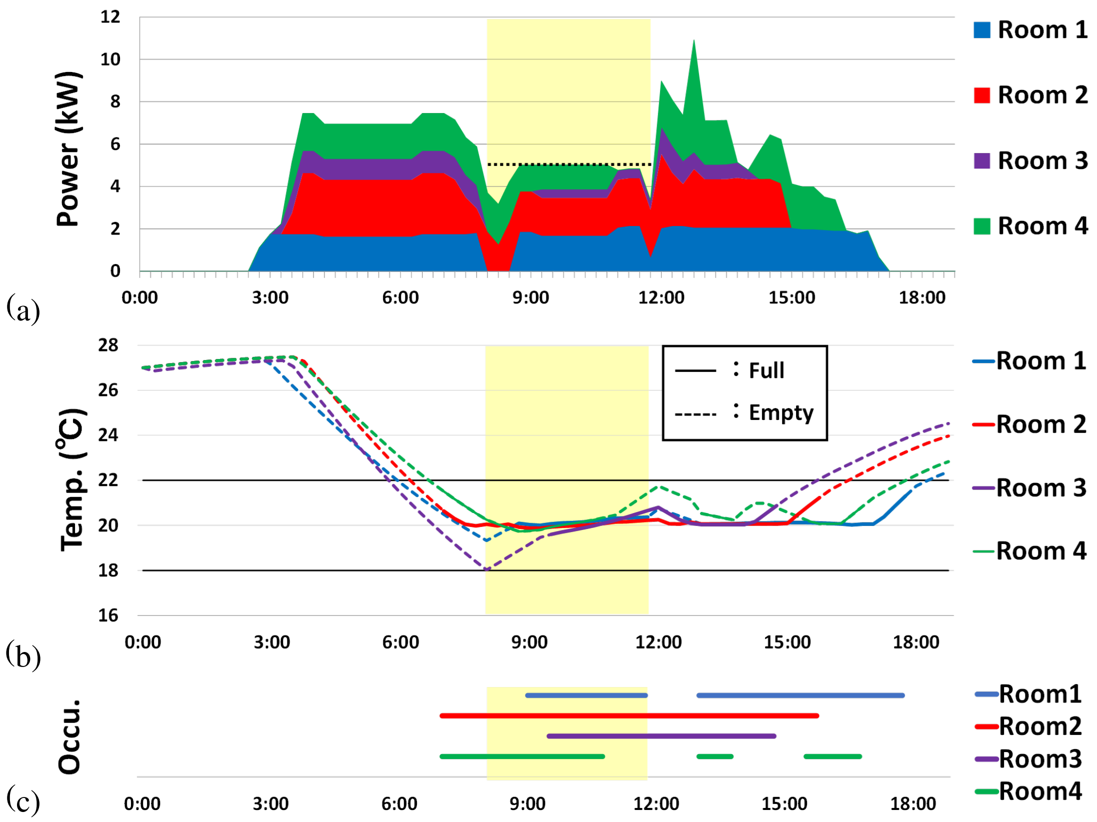

Figure 3.4: Simulation result for $K_{i,t}^{r+c}$: (a) power consumption and (b) indoor temperature, under (c) given occupancy schedule.

3.6 Summary

This chapter discusses the scheduling of multiple HVAC systems using an electrical power allocation technique. The power allocation technique calculates the amount of electrical power allocated to each HVAC system. The power allocation is done while considering power limitations, prior to HVAC scheduling. This calculation is based on factors such as the number of users and the capacity of the HVAC outdoor unit. In this chapter, power limitations are considered specifically to facilitate load shedding and shifting. In the simulations, a scenario is considered where the total electrical power of the HVAC is limited to 21.7% of its maximum value. In the experiment, it was observed that the proposed method successfully schedules for each HVAC system while keeping power limitation and maintaining thermal comfort. With respect to contribution to the demand-supply balance, the proposed method allows for the reduction of a building's peak power by accounting for power constraints across multiple HVAC systems. Regarding GEBs, this approach significantly contributes to load shedding/shifting strategies (Table 1.1) within the GEB framework. This is achieved by integrating the proposed method with HVAC aggregation techniques.

Chapter 4

Flexibility Price Forecasting for Ancillary Service Market

Grid-interactive efficient buildings (GEBs) used to just consume electricity, but now they play a more active role in the market that balances supply and demand. This makes energy systems more flexible. In order to make more GEBs' revenue, accurate market price forecasts and energy bids for supply and demand balancing markets are called frequency control ancillary service (FCAS) markets. Forecasting FCAS market prices is complex due to the presence of various response time markets and the interdependence of markets, where one price has a direct or indirect impact on others. There is a lack of studies on forecasting electricity prices in FCAS markets. Therefore, it is necessary to develop a novel forecasting model that takes into account not only the price of the target market but also the prices of other response time markets. In this chapter, a new model is presented to forecast market prices in the Frequency Control Ancillary Services (FCAS) market. This model is based on forecasting methods from the wholesale market. This model also considers markets with different response times, including the forecast target market overseen by the Australian Energy Market Operator (AEMO). The experimental results show that the developed forecasting model achieved an RMSE of 7.8\$/MWh in the AEMO 6-Second-Raise market. The developed forecasting model improves accuracy, reducing the RMSE by 80% compared to the forecast prices issued by the AEMO.

4.1 Introduction

In the quest for societal decarbonization, GEBs have emerged as a promising avenue to improve the stability of the grid. Participation of GEBs in supply and demand balancing markets necessitates precise prediction of market transaction prices. These predictions are crucial for developing strategies that enable optimal bidding of electrical flexibility by GEBs, thereby maximizing revenue and fostering efficient energy supply methods.

Nevertheless, to the best of the author's knowledge, there is a lack of research on electricity price forecasting in FCAS markets.

AEMO operates as a public company in Australia, managing both the wholesale and FCAS markets. In these markets, demand-side participation is allowed for power dealings aimed at frequency control. The FCAS market is segmented by response times and categories like raise and lower. These segments have a complex interplay, making electricity price forecasting more challenging. Currently, there is a notable absence of research focused on forecasting prices within the FCAS market.

The FCAS market is reported to have pricing policies and characteristics similar to those of the wholesale electricity market [87]. Previous research in spot price forecasting highlights the crucial role of selecting suitable learning models and implementing effective data pre-processing techniques to enhance the accuracy of predictions [59, 88–92]. Based on these studies, this research introduces a framework for forecasting prices in the FCAS market.

This chapter delves into developing a forecasting model for the FCAS market, building upon prior research in the wholesale electricity market. The exploration is segmented into three key areas affecting forecast accuracy: learning models, data pre-processing, and the selection of input data. Each segment's forecast accuracy was assessed to determine the most effective design for the FCAS market. The key contributions of this chapter are outlined below.

- The forecasting model for the FCAS market is designed by leveraging approaches from the wholesale market and incorporating data from FCAS markets with varied response times.
- The forecasted prices from the designed model are more accurate compared to those published by the AEMO, as evidenced by a 80% reduction in forecast error, measured by the RMSE.

4.2 Related Research

The research presented in this chapter is clearly a very novel and, as yet, less active research domain where few existing papers are available. So, there has been a notable absence of studies focused on price forecasting within supply and demand balancing markets. This part initially presents research on DER management, highlighting the need for market forecasting. Subsequently, it delves into literature that analyzes and forecasts markets highly relevant to balancing markets.

Numerous studies have delved into the management of DERs within aggregators. More recently, the focus has expanded not only to managing DERs but also to coordinating their bidding in the market. Naughton et al. [93] assumed that market transaction prices were known and proposed DER management techniques based on this information. Some research [42, 43] dissected aggregator activities into DER management and pre-bidding concerns. Studies involving bidding problems optimized pre-bidding strategies using predicted prices derived from market price signals. However, discrepancies between these signals and actual transaction prices led to losses for aggregators and consumers. Therefore, there is a crucial need for methods that accurately predict transaction prices in the supply-demand balancing market rather than relying solely on price signals.

Existing research [87, 94, 95] detailing the mechanics of these markets has highlighted the characteristic price fluctuations in this domain. Basically, it has been observed that the supply-demand balancing market and the wholesale electricity market have similar price trends due to contractual agreements based on the balance between supply and demand. However, the supply-demand balancing market, responsible for fine-tuning electricity supply and demand after the closure of the wholesale electricity market, experiences significantly more severe price fluctuations, making predictions challenging. In light of these insights, it is proposed to take advantage of knowledge from the wholesale electricity market to construct a forecasting model for the electricity supply-demand balancing market. The primary goal is to improve the accuracy of the forecasts in the electricity supply-demand balancing market. To do this, it is necessary to identify the key components that support accurate forecasting in the wholesale electricity market and incorporate them into the model's development.

4.3 System Model

This chapter considers six FCAS markets with different response times operated by AEMO. The FCAS markets play a crucial role in ensuring the stability of the grid by maintaining the balance between supply and demand. Their primary objective is to keep the frequency of the grid within national standards. The FCAS market is divided into two categories: "raise" and "lower." The raise FCAS is specifically designed to address frequency drops by increasing either the energy generation or decreasing demand. In contrast, the Lower FCAS is intended to manage an increase in frequency by reducing energy generation or increasing demand. Based on response times, the FCAS market is classified into three types: fast services (6 seconds), slow services (60 seconds), and delayed services (5 minutes). Thus, FCAS has six markets according to the type of market and response time. AEMO uses data from two primary sources to forecast prices in the FCAS market: FCAS market data, which includes FCAS dispatch prices, and AEMO wholesale market data, which includes demand, generation, and spot prices [96].

The forecasting system proposed in this research is shown in Figure 4.1. As shown in Figure 4.1, FCAS market prices and the wholesale market data are used as input data. A detailed description of the input is shown in Table 4.1. The reason for using the wholesale market is that it is known that incorporating correlated inputs, such as electricity prices from neighboring countries, can significantly enhance the accuracy of forecasts [88]. Figure 4.2 shows the price variations over a week in the Raise markets,

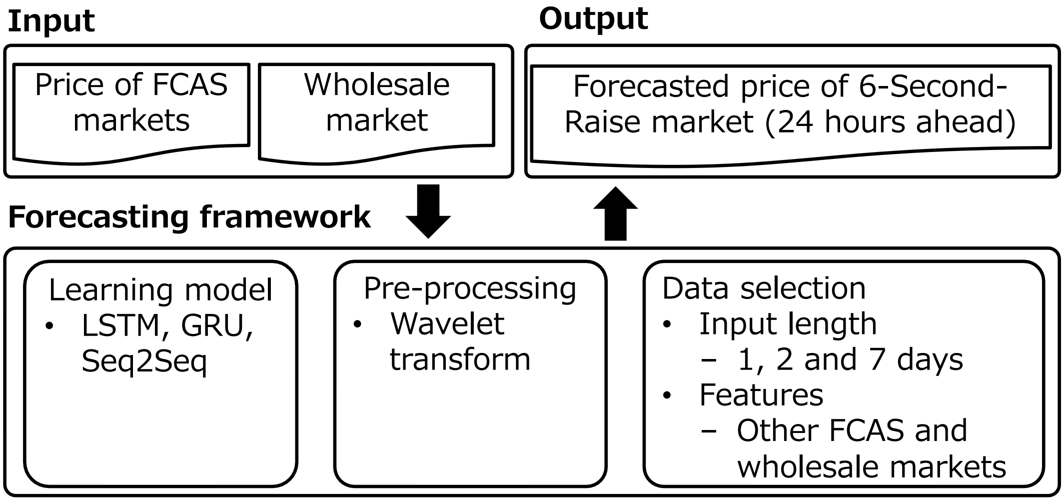

Figure 4.1: Overview of forecasting system

Table 4.1: The data of six FCAS market and wholesale market

FCAS market	Price of 6-Second-Raise (6SR) market Price of 60-Second-Raise (60SR) market Price of 5-Minute-Raise (5MR) market Price of 6-Second-Lower (6SL) market Price of 60-Second-Lower (60SL) market Price of 5-Minute-Lower (5ML) market
Wholesale market	Spot price (S-price) Total demand (Demand) Total generation (Generation)

highlighting the differences between various response time categories. As shown in Figure 4.2, raise markets show synchronized price fluctuations. It is significant to note that the AEMO published the data used in this research, making them practically accessible.

The forecasting framework consists of three primary components: the learning model, pre-processing methods, and the selection of input data. It is widely acknowledged that the learning model significantly influences the accuracy of the forecasts [89]. In order to improve the accuracy of forecasts, wavelet transforms are utilized as a data pre-processing method. Iwabuchi et al. show that this technique has been shown to be effective for forecasting demand in the wholesale market [90]. In the FCAS market, forecast accuracy can be improved by carefully selecting the input data from the prices of the six contingency markets, each with its own distinct response time.

This chapter addresses the forecast of the *6-Second-Raise (6SR) market*, which had the highest average price and yearly transaction price among the FCAS market in 2021. The reason for this is that accurate predictions in such markets enable GEBs to improve

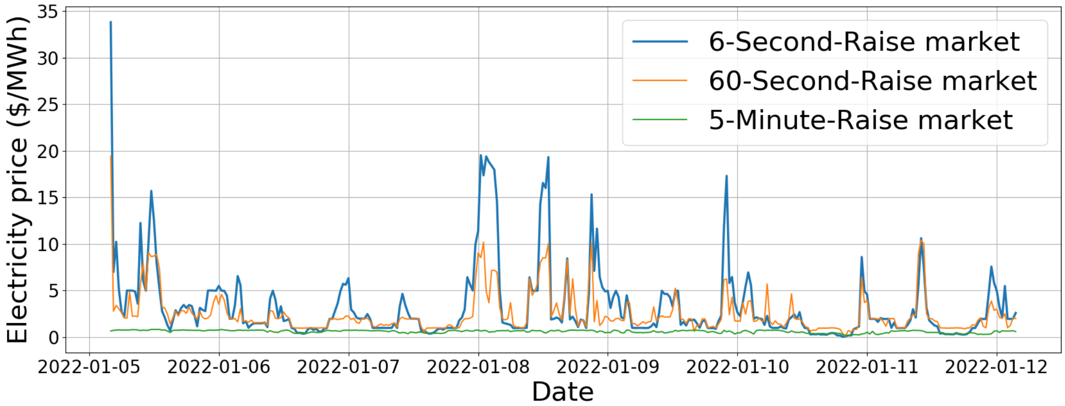

Figure 4.2: Price profiles in FCAS raise markets

their financial returns. The proposed framework forecasts prices in the FCAS 6-Second-Raise market with 24 hours ahead. This market is recognized as a market for bidding flexibility, as evidenced by several researches [42, 43, 93]. It should be noted that the forecasting framework developed in this research is versatile and can be adapted to other FCAS markets.

4.4 A Framework of Price Forecasting

This section outlines the specifics of the three main components within the framework: the learning model, data pre-processing, and input data selection. Each component of the proposed framework has been previously explored in the wholesale electricity market. This chapter applies these components to the forecasting framework for FCAS markets.

4.4.1 Learning Model

This chapter focuses on forecasting the time series of prices within the FCAS market. In this framework, recurrent neural networks (RNNs), which are effective for analyzing time series data, along with the sequence-to-sequence (Seq2Seq) architecture, known for its capabilities in time-series forecasting, are utilized. These methods are chosen for their proficiency in handling and predicting data trends over time.

RNNs: RNNs have loops in their structure, enabling them to retain information. This feature is particularly useful for modeling time-series data. RNNs differ from multilayer perceptrons as they utilize the temporal aspects of input data, making them more suited for time series forecasting. LSTM networks, which are an improvement on RNNs, fix the vanishing gradient problem that RNNs often have by adding memory cells to their hidden layers. These memory cells aid in preserving information over longer periods, enhancing the model's ability to handle time series data effectively. Zhou et al. used LSTM as a more accurate prediction model than traditional RNNs [91]. Gated recurrent unit (GRU) is recognized as a more compact and faster alternative to LSTM the LSTM [92].

Seq2Seq for RNN: Seq2Seq, a neural network architecture, comprises two primary components: an encoder and a decoder. The encoder processes a series of input data and converts it into a fixed-length representation known as the context vector. This context vector is then passed to the decoder, which generates a corresponding output sequence. Seq2Seq models are particularly useful in long-term forecasting applications, where they can effectively translate input sequences into meaningful future predictions. Sridharan et al. [89] utilized an LSTM-based encoder-decoder model to forecast spot prices in the wholesale market. Their study indicates that the incorporation of LSTM or GRU cells within the Seq2Seq architecture makes it better at forecasting time series data. In this chapter, the performance of three different recurrent neural network models and their combinations with the Seq2Seq model are compared to evaluate their accuracy.

4.4.2 Pre-processing

While normalization is a standard practice in deep learning pre-processing, this research focuses on leveraging frequency decomposition. Frequency decomposition is recognized for its effectiveness in improving time series data forecasting, offering a strategic advantage in analyzing and predicting complex patterns.

Wavelet Transformation: Wavelet analysis starts by selecting an appropriate wavelet, often referred to as the mother wavelet. The analysis then proceeds by examining translated and dilated versions of this selected wavelet. This process forms the core of the wavelet analysis methodology. The wavelet transform technique breaks down the original time series into several subcomponents. This decomposition reduces the complexity of the data, making it easier to analyze and forecast. Iwabuchi et al. [90] achieved to improve precision in their price forecast models by switching various mother wavelets. In identifying the most effective mother wavelets for forecasting FCAS market price data, this research draws on insights from previous studies.

4.4.3 Input Data Selection

This chapter assumes six FCAS markets, each with a different time series of price data. The input length and the features of the input data can be selected.

Input length: In time series forecasting, the input length, which refers to the number of historical data points used as input for the forecasting model, is a key factor. The forecast accuracy in this model is significantly influenced by the input length, largely because the model complexity is dependent on this factor. The time series analysis of daily prices on the wholesale electricity market indicates a significant correlation between prices from the previous day, two days ago, and one week ago [59]. Consequently, this study also explores the impact of using three different input lengths on the accuracy of the forecast: one day, two days, and seven days from the past.

Markets for learning: Input data selection is a key topic in forecasting time series data. This focus is due to the fact that including highly relevant time series data can significantly improve the accuracy of forecasts. Therefore, FCAS market data are used as input, along with wholesale market data, as depicted in Table 4.1.

4.5 Experiments

In this research, the experiments involve exploring various combinations of factors within the forecasting framework to identify the most effective model in terms of forecast accuracy. The proposed framework forecasts the electricity price of the *6-Second-Raise (6SR) market* in FCAS. The choice of a learning model is essential for exploring an effective forecasting framework. Initially, a comparison is made between models using RNN, LSTM, and GRU, with or without the Seq2Seq architecture, to choose the optimal model that achieves the highest level of forecast accuracy. Furthermore, the optimal model undergoes pre-processing using several mother wavelets and is subsequently compared. Thus, the forecasting framework is identified, achieving the best accuracy in forecasting. Finally, the effectiveness of the forecasting model is demonstrated by comparing its forecasting results with AEMO's pre-dispatch prices as a benchmark. Pre-dispatch prices are utilized as inputs in research focusing on demand-side optimization [42, 93]. In other words, achieving a forecast price accuracy that surpasses the pre-dispatch price suggests that GEBs could potentially increase their revenue. To the best of author's knowledge, this research is the first to design a price forecasting model for FCAS markets. Hence, due to the lack of existing research specifically on electricity price forecasting in FCAS markets, there is no state-of-the-art work for comparison other than AEMO pre-dispatch.

4.5.1 Setup

For historical FCAS market prices, this chapter used AEMO's dispatch prices from 2021 as a reference. The data series was recorded at 30-minute intervals. The forecasting framework was designed to predict prices 24 hours ahead every 30 minutes, similar to AEMO's pre-dispatch process. In these experiments, the forecasting involves a weekly repetition of time series decomposition and learning. The model's training, validation, and testing phases are structured over specific periods: it trains on four weeks of data, validates on one week, and tests on the next week. For instance, testing takes place from January 5 to 11 of 2022 after training using price and demand data from December 1-28 of 2021, and validation with data from December 29, 2021, to January 4, 2022. The process is iterated, with the data being shifted by one week in each iteration, for a total

Table 4.2: Forecasting performance across different models

Model name	**MAE**	**RMSE**	Var_{score}	Max
RNN	6.81	13.2	-16.0	857
LSTM	5.60	12.1	-15.8	836
GRU	6.00	12.3	-16.2	866
RNN-Seq2Seq	3.85	9.56	-0.82	357
LSTM-Seq2Seq	**3.67**	**9.54**	**-0.14**	**356**
GRU-Seq2Seq	3.68	10.1	-0.89	363

Table 4.3: Forecasting performance across different mother wavelets

Mother wavelet	**MAE**	**RMSE**	Var_{score}	Max
w/o Wavelet	3.67	9.54	-0.14	356
Daubechies 4	**3.55**	**8.63**	**0.02**	**355**
Daubechies 5	4.17	27.3	-8.74	2030
Daubechies 6	5.22	30.4	-11.1	1770
Symlet 5	4.59	21.5	-5.10	880

period of 16 weeks, resulting in a forecast of prices for 16 weeks. Adam is used as an optimizer.

The evaluation metrics used to assess the forecasting accuracy of the model are introduced. In the realm of price forecasting, the mean absolute error (MAE) and the root mean squared error (RMSE) are the main metrics employed to assess the efficacy of a model. Furthermore, the forecast performance of each model is evaluated using the variance regression score (Var_{score}) and the maximum residual error (Max). The model's accuracy in forecasting increases as Var_{score} approaches one and decreases as it becomes more negative. A lower value of Max suggests more precise forecasting.

4.5.2 Results

A comparison was made between six distinct models: *RNN*, *LSTM*, *GRU*, *RNN-Seq2Seq*, *LSTM-Seq2Seq*, and *GRU-Seq2Seq*. Initially, this research carried out a comparative analysis of forecast accuracy among different models. The six models employed input with *6SR* and 48 steps without utilizing wavelet transformation. Table 4.2 shows the forecast accuracy represented by each evaluation metric. When comparing regression models alone and those combined with Seq2Seq in Table 4.2, it is evident that the models integrated with Seq2Seq exhibit higher levels of accuracy. The model with Seq2Seq showed improved accuracy, attributed to its strength in forecasting long-term data. In this learning model exploration, *LSTM-Seq2Seq* was the suitable model to forecast the price of electricity in the FCAS market.

Subsequently, the forecasting accuracy of models based on *LSTM-Seq2Seq* was as-

Table 4.4: Forecasting performance across different input lengths

Input length	**MAE**	**RMSE**	Var_{score}	Max
48 steps (1 day)	**3.55**	**8.63**	**0.02**	**355**
96 steps (2 days)	4.02	9.88	-0.27	353
336 steps (1 week)	5.28	19.3	-3.84	1040

Table 4.5: Forecasting performance across different input markets

Markets	**MAE**	**RMSE**	Var_{score}	Max
6SR	3.55	8.63	0.02	355
6SR & 60SR	**3.41**	**7.80**	**0.12**	**330**
6SR & 5MR	4.34	16.7	-2.65	522
6SR & 6SL	4.67	24.2	-6.69	1320
6SR & 60SL	4.89	24.6	-6.94	1320
6SR & 5ML	4.55	18.1	-3.30	851
6SR & S-price	3.67	11.4	-0.71	919
6SR & Demand	5.25	36.7	-16.7	1620
6SR & Generation	5.71	38.5	-18.5	1680

sessed by comparing their performance using different mother wavelets. In this comparison, four types of mother wavelets — *Daubechies 4, 5, and 6 and Symlet 5* - were evaluated. These wavelets were selected based on their demonstrated accuracy in forecasting wholesale electricity market prices, as detailed in the previous study referenced in [90]. The terms "Daubechies" and "Symlet" refer to the primary wavelet functions, whereas the numerical value associated with each term is known as the vanishing moment. Table 4.3 shows the forecast accuracy compared with the mother wavelets. Based on this analysis of mother wavelets, it was determined that the *Daubechies 4* wavelet exhibited the best level of accuracy.

The impact of input length on accuracy was evaluated using the *LSTM-Seq2Seq* model with the *Daubechies 4*. The input lengths compared were 48 steps (equivalent to one day), 96 steps (equivalent to two days), and 336 steps (equivalent to seven days). The forecast accuracy with varying input length is shown in Table 4.4. The results revealed that forecasting accuracy decreased progressively as the input length increased, with optimal results observed using a 48-step input length. This finding suggests that using one day's worth of data is adequate for predicting prices over the next 24 hours.

Additionally, the accuracy of using learning features from different markets was assessed. It's uncertain how correlations between the FCAS markets and the wholesale electricity market may influence forecasting effectiveness. This experiment aims to clarify this particular aspect. The current findings indicate that the explored learning model is LSTM-Seq2Seq, the mother wavelet is Daubechies 4, and the input length is set to 48 steps. The accuracy was evaluated between some scenarios: one where only the target

(*6SR*) is used, and others where the target (*6SR*) is trained together with one of the data points from Table 4.1. The results obtained from various markets for learning features are presented in Table 4.5. The findings indicate that *6SR & 60SR*, which correspond to the same raise market but exhibit varying response times, were considered appropriate input for the forecasting framework owing to their small errors. Figure 4.2 clearly demonstrates the correlation between *6SR* and *60SR*. In this experiment, it is emphasized that the model design is founded on the *LSTM-Seq2Seq* architecture utilizing the *Daubechies 4*. The input data consisted of 48 sequential steps and included two distinct markets (*6SR* and *60SR*).

The price forecasts released by AEMO (*Pre-dispatch data set*) [96] and the explored forecast model for the *6SR* market were compared. Figures 4.3 and 4.4 show averages and forecast errors of forecasted prices, respectively, and contain actual prices and forecasting of the explored model and the pre-dispatch data set. The black line, blue line, and red line in Figure 4.3, respectively, represent the average daily prices of the actual prices and pre-dispatch data set and the prediction outcomes of the explored model. The blue and red lines in Figure 4.4, respectively, represent the daily RMSE of the pre-dispatch data set and the forecast outcomes of the explored model. The X-axis in Figures 4.3 and 4.4 represents the dates from January 1 to May 1 in 2022, and the Y-axis displays the daily average price and the daily RMSE, both measured on a logarithmic scale, indicating the power price. In general, the forecast accuracy for the entire period was 39.3 \$/MWh for AEMO's RMSE and 7.8 \$/MWh for the explored model, resulting in a reduction of 80. 2% in errors. When comparing their respective daily RMSE, Figure 4.4 shows that the explored model exhibits greater accuracy than AEMO's pre-dispatch data set. Figure 4.3 shows that during times of dramatic price increases, the pre-dispatch data diverged significantly from the actual market prices. In contrast, the forecast error of the explored model was minimal under these conditions. As a result, the overall prediction error of the explored model is lower than the overall error of the pre-dispatch data set.

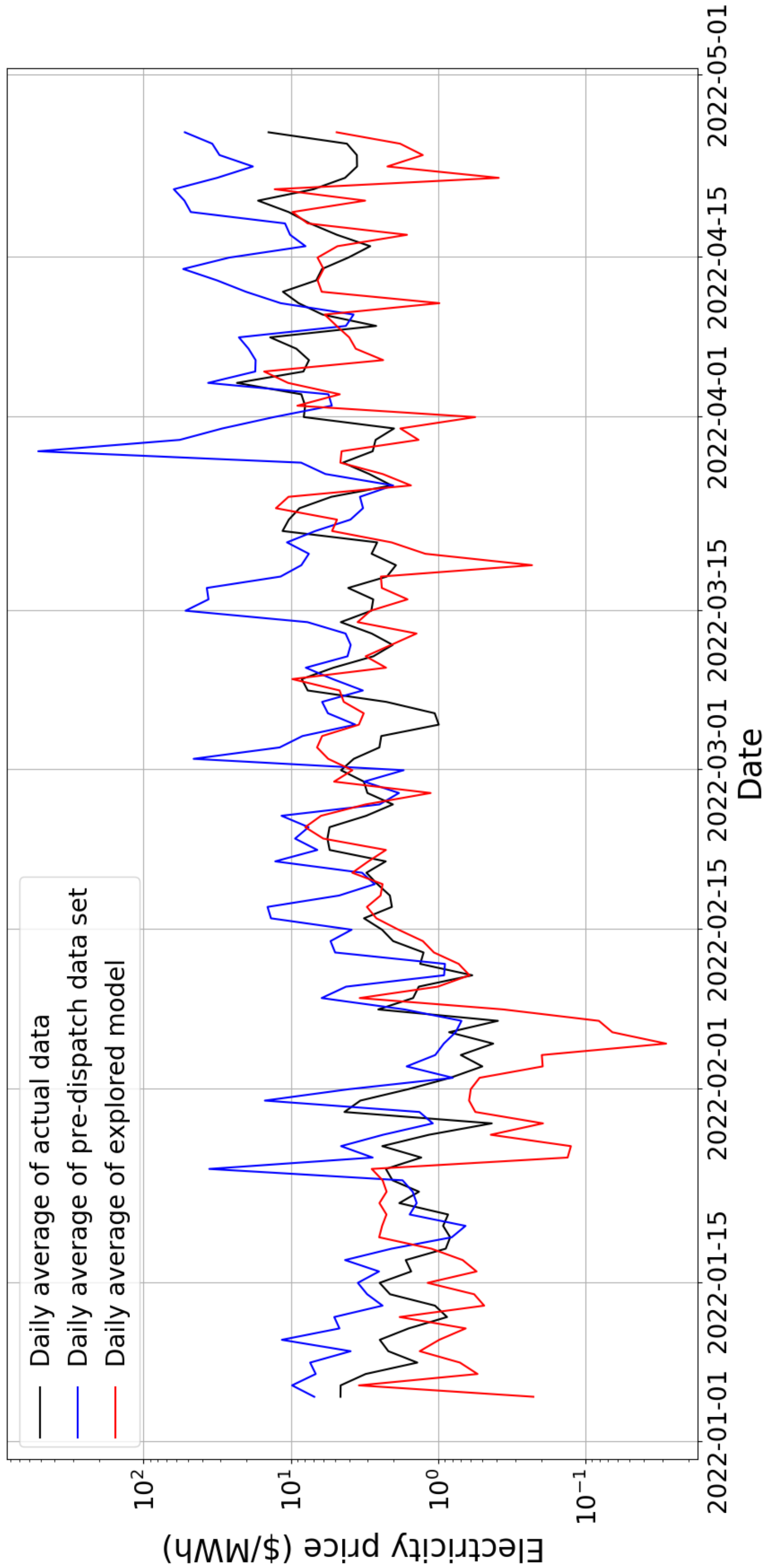

Figure 4.3: Daily average prices of actial, pre-dispatch data set, and explored model

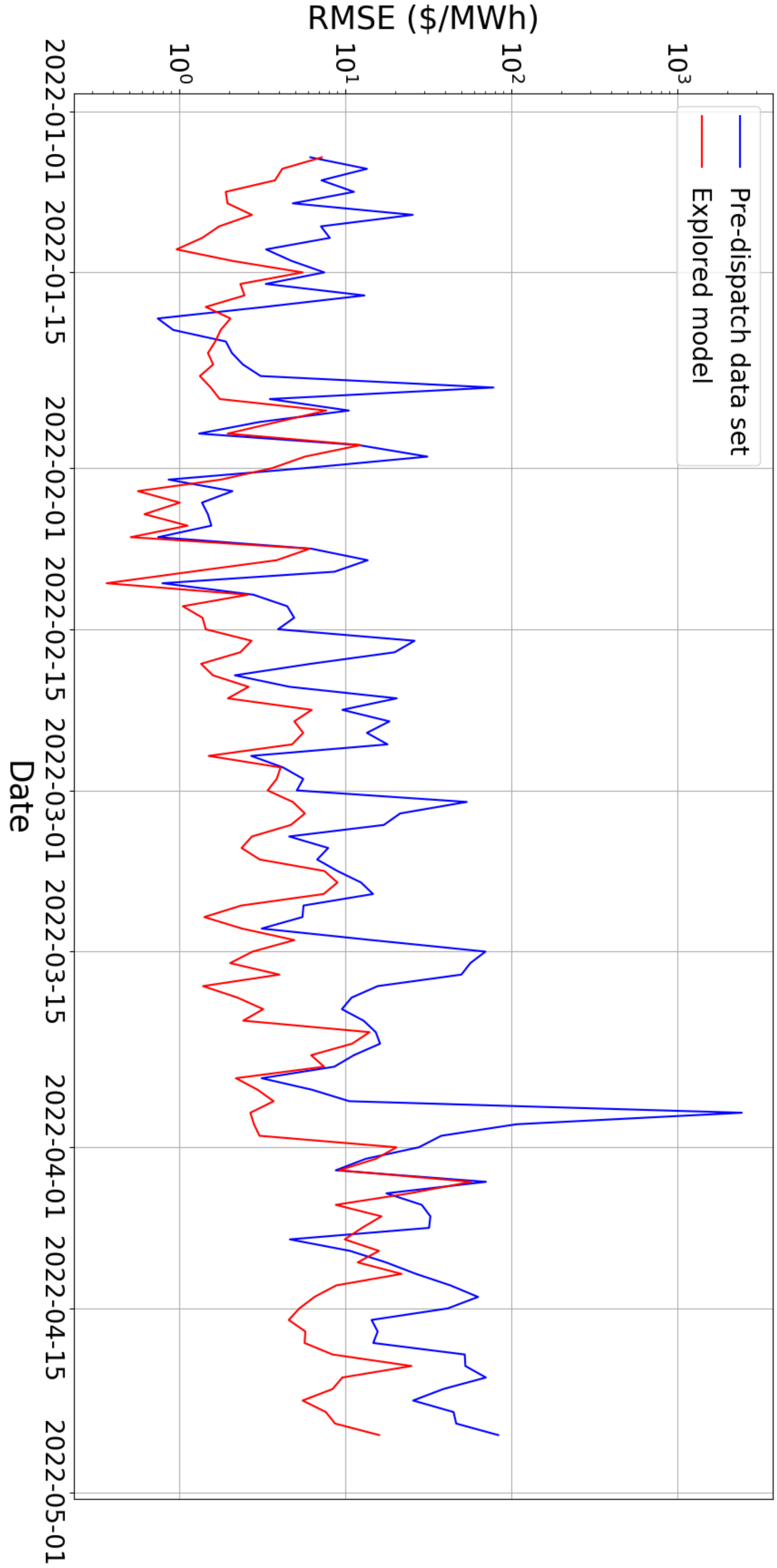

Figure 4.4: Daily RMSE of pre-dispatch data set and explored model

4.6 Summary

In this chapter, price forecasting models have been explored for the FCAS market. The evaluations were carried out on several components of the learning models, preprocessing, input length, and input markets, drawing from prior research on the wholesale market. The best forecasting models were compared with the forecast prices published by AEMO, and the results showed that the proposed model performed better than AEMO's pre-dispatch prices with a reduction of RMSE by 80%. The contribution of this research to GEBs lies in enabling more effective profit generation for GEBs participating in the supply and demand balancing market through more accurate price forecasting than conventional public data.

Chapter 5

Conclusion and Future Work

5.1 Conclusion

The increasing presence of variable and uncontrolled renewable energy requires flexible energy systems to address challenges such as demand-supply mismatches and high ramp rates. A promising solution is grid-interactive efficient buildings (GEBs), which allow altering building demand loads based on occupants and the conditions of the power grid. Within GEBs, distributed energy resources (DERs) on the demand side, such as battery systems and controllable demand, can be managed and coordinated using energy management methods. This dissertation focuses on addressing the grid-interactive efficient building aspect of the problem to improve the supply-demand balance. To harness the full potential of GEB, this dissertation addresses the three research questions outlined in Chapter 1.

5.1.1 Answer to Question 1: How can GEBs be used to effectively utilize surplus PV generation from the viewpoint of storage?

To optimize renewable energy utilization in GEBs, efficient ways to utilize generated power beyond internal consumption or the reverse flow of the grid are essential. Chapter 2 explores the utilization method of electric vehicles (EVs) in GEBs, presenting a method to redistribute excess renewable energy among buildings without relying on reverse power flow. The approach involves designated charging and charging facilities for EVs, along with EV aggregators. Each building plans its battery charging/discharging to minimize power costs, while the EV aggregator sets power trading prices based on individual building power sufficiency. This collaborative operation uses surplus power, increasing electricity flexibility through the EV aggregator. Experimental results demonstrate a significant reduction in wasted energy, achieving up to a 68% decrease in solar energy waste in the best-case scenario. In the same case, there has been a 14% reduction in purchased energy from the grid. The contribution of the EV aggregator to the demand-supply balance includes the temporal and spatial shifting of surplus generated power, which traditionally had to be discarded, thereby contributing to the reduction of purchased power for buildings. If the results of this experiment can be extended to entire residential and nonresidential buildings, which account for 30% of global final energy, it could lead to a reduction in energy demand ranging from 0.3 to 5.4% across the entire grid. IEA states that an 8% reduction in demand is necessary by 2050 to achieve Net Zero [97]. Although this experiment represents an ideal case, a maximum reduction of 5.4% is a significant contribution. Regarding the contribution to GEBs, this research proposes a new utilization of power by sharing it among buildings without relying on the power grid, which was previously only temporarily shifted within a building. By spatiotemporal energy shifting through the EV aggregator, it prevents reverse power flow from buildings to the grid, allowing more grid-conscious energy management. Additionally, with further development of this research and the exploration of new applications for generated power, it is expected that the optimal capacity of generation equipment that can be installed in GEBs will increase significantly. IRENA indicates that to reduce CO2 emissions, solar power generation needs to increase from 1053 GW to about 8000 GW by 2050 [98]. In the US, the current solar power capacity is only about 4 MW [4], but the U.S. department of energy's national renewable energy laboratory has noted that the potential solar power capacity installable on buildings can be extended up to 1000 GW [99]. The growth of EV aggregator technologies discussed in this chapter may be a key to achieving this potential.

5.1.2 Answer to Question 2: How can GEBs schedule DER operations considering peak power and building comfort from the viewpoint of consumption?

To achieve GEBs, it is essential to efficiently manage multiple HVAC systems, considering power usage constraints. Previous studies explored management using mathematical models like MPV and, more recently, delved into reinforcement learning approaches. However, managing numerous HVACs through model predictive control (MPC) often led to increased computation time, and reinforcement learning faced challenges due to data scarcity. Chapter 3 presents an MPC-based optimization method for the operation of multiple HVAC units that avoids computational delays. The proposed technique allocates available power resources to each unit based on power limits and obtains individual operation plans using edge devices owned by the respective HVAC systems. Experimental results show the effectiveness of this method, ensuring schedules for HVAC systems without exceeding power limits or compromising thermal comfort. Regarding contribution to the demand-supply balance, the proposed method allows for the reduction of a building's peak power by accounting for power constraints across multiple HVAC systems. Regarding GEBs, this approach significantly contributes to load shedding and shifting strategies (Table 1.1) within the GEB framework. By combining the proposed method with HVAC aggregation techniques, this is possible. Additionally, as this research advances to accommodate power constraints among HVAC systems in various usage scenarios and buildings, there is hope for new possibilities. The expectation is that this will enable the creation of flexibility by freely interconnecting HVAC systems, regardless of their spatial locations. It is suggested that the power consumption of air conditioning systems within buildings accounts for about 13.5% of the global final energy consumption [9]. When the proposed approach is further developed for entire buildings, 10% of the HVAC power capacity can be shifted or reduced, which indicates that 1.35% of the total electricity demand can be treated as flexibility. In the net zero scenario, by 2030, it is necessary to implement approximately 250 GW of demand response capacity in buildings, yet currently only about 20 GW has been achieved [97, 100]. Therefore, the advancement of this research is important for stabilizing the future supply-demand balance.

5.1.3 Answer to Question 3: How can GEBs predict the transaction price of electrical flexibility for efficient interaction with the market?

In the realm of GEBs, the focus has traditionally been on energy management for tasks like load shifting and load balancing. Recently, research has expanded to include creating electrical flexibility, aiming to balance electricity supply and demand. However, many studies overlook the financial aspects of market transactions. Notably, there's a scarcity of research on forecasting transaction prices in the supply-demand balancing market, where flexibility is bought and sold. Chapter 4 addresses this gap by constructing a transaction price forecasting model for the electricity supply-demand balancing market. The model integrates market price forecasting with data from other commodity categories and wholesale electricity market transactions to enhance GEB's profitability. Evaluation experiments resulted in accurate predictions of the AEMO 6-Sec-Raise market price, achieving an RMSE of 7.8$/MW, which is an 80% improvement over the RMSE of AEMO's provided data. By combining this forecasting model with existing energy management methodologies, GEB can expect stable remuneration from its participation in the supply-demand balancing market. In the future, this research will stabilize the rewards of flexibility for GEBs, and it is expected that the number of GEBs participating in the market will increase. Consequently, this could lead to an increase in the total amount of demand-side flexibility.

5.2 Future Work

The works presented in this dissertation will be able to extend in several directions.

Enhanced EV Aggregator Pricing Algorithm

In Chapter 2, GEBs decision-making was optimized to determine whether to buy or sell in response to the pricing set by the EV aggregator. However, in reality, consumers often have their own decision criteria, known as price elasticity, which influences their willingness to buy or sell based on the price. Therefore, future optimization methods need to consider price elasticity on the consumer side, and pricing algorithms on the EV aggregator side should factor in household price elasticity when determining purchase and sale prices.

Integrating Supply-Demand Balancing Capabilities into EV Aggregators

In Chapter 2, EV aggregators were primarily involved in power transactions between buildings, buying and selling power to facilitate energy transfer. The assumption was that these aggregators would purchase electricity from the grid when their batteries were low and feed excess power back to the grid when recharging was not possible. In other words, the EV aggregator does not anticipate trading electricity with the market through battery charge/discharge. However, recent advances have allowed electric vehicle aggregators to participate in the supply-demand balancing market. Consequently, future EV aggregators should be equipped to engage in the supply-demand balancing market, enabling them not only to facilitate power transfers but also to generate balancing power when necessary.

Adapting EV Aggregators to Human and Environmental Complex Factors

In Chapter 2, this chapter used a simple household model. However, when considering real-world scenarios, it is necessary to factor in constraints originating from human behavior and environmental conditions. This is crucial because human activities can significantly impact the use of EVs, the energy budget, and the demand predictions used in the proposed framework. Consequently, these factors could potentially lead to errors in classifying households based on the energy budget, as well as in transactions of electricity between EVs and EV aggregators. Therefore, developing methods that take into account human and environmental constraints is an important future direction.

Challenges in Introducing EV Aggregators in the Real World

In Chapter 2, the most significant challenge in practical implementation of the proposed EV aggregator is predicting the "energy budget," a critical factor in price determination. This chapter proposes a method under the assumption that generation power and household demand can be predicted. However, environmental factors cause generated power to fluctuate significantly, and residents' impulsive behavior has a significant impact on EV and household demand predictions. These factors add complex constraints to the proposed method, making its application in the real world challenging. To address these issues, more accurate prediction methods and strategies that consider the uncertainty in the energy budget due to prediction errors are needed. The energy budget is used as an indicator to understand the energy balance of each household. Therefore, it might be possible to cluster households based on predictive information and past transaction data regarding energy balance. The use of this clustering information could potentially solve the challenges associated with predicting the energy budget.

Scaling up HVACs Management to Building Level

In Chapter 3, multiple HVAC optimizations were performed for only four rooms. However, to realize GEB, it is essential to consider the number of HVAC units at the building level. Therefore, in future research, it is imperative to assess the scalability through simulations at the building level using the proposed methodology. By integrating the proposed methodology with appropriate HVAC aggregation techniques, a comprehensive framework for energy management in buildings can be provided.

Load Shifting Using the Proposed Methodology Considering GEB's Base Load Assumptions

In Chapter 3, the simulations were conducted under the assumption of power restrictions imposed on available power for HVACs. However, in GEB, there are other base loads to consider, not just HVACs. Therefore, the power constraints allocated to HVACs must be determined based on both the building's power limits and the base demand. Hence, future research needs to evaluate the effectiveness of the proposed methodology using real datasets from operational GEB scenarios.

Application of the Proposed Methodology to Other Markets

In Chapter 4, a specific focus was given to predicting transaction prices in the AEMO 6 Second-Raise market. However, the supply-demand balancing market comprises various market segments beyond the 6 Sec Raise market. Predictions for these markets are equally vital information for participation in the supply-demand balancing market. Therefore, it is necessary to apply the proposed methodology to other market segments and evaluate the accuracy of price forecasts.

Price Forecasting Method Considering Other Market Participants

In Chapter 4, the current method forecasts prices based on past information from the supply and demand balancing market and the wholesale electricity market. However, when considering actual bidding in the market based on these forecasts, it is essential to take into account information about other market participants. For example, if price forecasting indicates high transaction prices at certain times, other participants will likely also bid during those times. Consequently, the market clearing price may end up being lower. The actions of other participants can significantly influence market prices. Therefore, the forecasting method for the transaction prices of flexibility that takes into account such dynamic information, including the behavior of other participants, should be investigated in the future.

Coordination Between the Prediction Model and Aggregator's Bidding Strategy

In Chapter 4, transaction price predictions in the supply-demand balancing market were conducted, and their effectiveness was evaluated based on the accuracy of these forecasts. The objective of this study is to increase the rewards obtained by GEBs and aggregators. To enhance the aggregator's rewards, studies have been conducted on the optimization of the aggregator's bidding strategies. Hence, it is necessary to assess the effectiveness of the proposed prediction method through simulations utilizing these bidding and prediction techniques.

Bibliography

[1] United Nations, "Global sustainable development report 2023," https://sdgs.un.org/gsdr/gsdr2023, 2023, accessed: 2023-11-07.

[2] I. Dincer, "Renewable energy and sustainable development: A crucial review," *Renewable and Sustainable Energy Reviews*, vol. 4, no. 2, pp. 157–175, 2000.

[3] N. L. Panwar, S. C. Kaushik, and S. Kothari, "Role of renewable energy sources in environmental protection: A review," *Renewable and Sustainable Energy Reviews*, vol. 15, no. 3, pp. 1513–1524, 2011.

[4] IRENA, *Renewable Energy Statics 2022*. The International Renewable Energy Agency (IRENA), 2022.

[5] H. Ritchie, M. Roser, and P. Rosado, "Energy," *Our World in Data*, 2022.

[6] N. Phuangpornpitak and S. Tia, "Opportunities and challenges of integrating renewable energy in smart grid system," *Energy Procedia*, vol. 34, pp. 282–290, 2013.

[7] S. R. Sinsel, R. L. Riemke, and V. H. Hoffmann, "Challenges and solution technologies for the integration of variable renewable energy sources — a review," *Renewable Energy*, vol. 145, pp. 2271–2285, 2020.

[8] B. Glensk and R. Madlener, "The value of enhanced flexibility of gas-fired power plants: A real options analysis," *Applied energy*, vol. 251, p. 113125, 2019.

[9] G. A. for Buildings and Construction, "2021 Global Status Report for Buildings and Construction," https://globalabc.org/sites/default/files/2021-10/GABC_Buildings-GSR-2021_BOOK.pdf, [Online; accessed 16-Dec-2023].

[10] S. Østergaard Jensen, A. Marszal-Pomianowska, R. Lollini, W. Pasut, A. Knotzer, P. Engelmann, A. Stafford, and G. Reynders, "Iea ebc annex 67 energy flexible buildings," *Energy and Buildings*, vol. 155, pp. 25–34, 2017.

[11] M. Neukomm, V. Nubbe, and R. Fares, "Grid-interactive efficient buildings," 2019.

[12] I. E. A. (IEA), "Efficient Grid-Interactive Buildings Future of buildings in ASEAN," https://iea.blob.core.windows.net/assets/71d1b69d-e8aa-49e5-9e0c-12c13d5a3a1f/EfficientGrid-InteractiveBuildings.pdf, [Online; accessed 29-Dec-2023].

[13] H. Li, Z. Wang, T. Hong, and M. A. Piette, "Energy flexibility of residential buildings: A systematic review of characterization and quantification methods and applications," *Advances in Applied Energy*, vol. 3, p. 100054, 2021.

[14] Z. Liu, Q. Ma, Y. Luo, L. Cheng, Y. Yuan, H. Qi, Z. Zhang, and T. Lu, "Economic analysis of grid-interactive efficient buildings: A case study in south china," in *2022 IEEE 6th Conference on Energy Internet and Energy System Integration (EI2)*, 2022, pp. 2487–2492.

[15] Y. Ye, C. A. Faulkner, R. Xu, S. Huang, Y. Liu, D. L. Vrabie, J. Zhang, and W. Zuo, "System modeling for grid-interactive efficient building applications," *Journal of Building Engineering*, vol. 69, p. 106148, 2023.

[16] S. Rahman, A. Haque, and Z. Jing, "Modeling and performance evaluation of grid-interactive efficient buildings (geb) in a microgrid environment," *IEEE Open Access Journal of Power and Energy*, vol. 8, pp. 423–432, 2021.

[17] M. Steen and M. Krarti, "A review and categorization of grid-interactive efficient building technologies for building performance simulation," *Journal of Engineering for Sustainable Buildings and Cities*, vol. 1, no. 4, p. 040801, 2020.

[18] Y. Wang, Y. Xu, and Y. Tang, "Distributed aggregation control of grid-interactive smart buildings for power system frequency support," *Applied Energy*, vol. 251, p. 113371, 2019.

[19] E. Vindel, M. Bergés, B. Akinci, O. Kavvada, and V. Gavan, "Alphashed: A scalable load flexibility model for shedding potential in commercial hvac systems," *Energy and Buildings*, vol. 279, p. 112686, 2023.

[20] H. Xu, I. Kanaya, S. Hiura, and K. Sato, "User interface by real and artificial shadow," in *ACM SIGGRAPH 2006 Research Posters*, ser. SIGGRAPH '06. New York, NY, USA: Association for Computing Machinery, 2006, p. 83–es.

[21] W. Turner, I. Walker, and J. Roux, "Peak load reductions: Electric load shifting with mechanical pre-cooling of residential buildings with low thermal mass," *Energy*, vol. 82, pp. 1057–1067, 2015.

[22] X. Yuan, Y. Pan, J. Yang, W. Wang, and Z. Huang, "Study on the application of reinforcement learning in the operation optimization of hvac system," *Building Simulation*, vol. 14, no. 1, pp. 75–87, 2021.

[23] L. Yu, Y. Sun, Z. Xu, C. Shen, D. Yue, T. Jiang, and X. Guan, "Multi-agent deep reinforcement learning for hvac control in commercial buildings," *IEEE Transactions on Smart Grid*, vol. 12, no. 1, pp. 407–419, 2021.

[24] C. Fu and Y. Zhang, "Research and application of predictive control method based on deep reinforcement learning for hvac systems," *IEEE Access*, vol. 9, pp. 130 845–130 852, 2021.

[25] P. Finn, M. O'Connell, and C. Fitzpatrick, "Demand side management of a domestic dishwasher: Wind energy gains, financial savings and peak-time load reduction," *Applied Energy*, vol. 101, pp. 678–685, 2013, sustainable Development of Energy, Water and Environment Systems.

[26] S. Farzamkia, H. Ranjbar, A. Hatami, and H. Iman-Eini, "A novel pso (particle swarm optimization)-based approach for optimal schedule of refrigerators using experimental models," *Energy*, vol. 107, pp. 707–715, 2016.

[27] M. Glavan, D. Gradišar, I. Humar, and D. Vrančić, "Refrigeration control algorithm for managing supermarket's overall peak power demand," *IEEE Transactions on Control Systems Technology*, vol. 27, no. 5, pp. 2279–2286, 2019.

[28] R. Torkzadeh, H. R. Chamorro, R. Rye, M. Eliassi, L. Toma, and F. Gonzalez-Longatt, "Reactive power control of grid interactive battery energy storage system for wadc," in *2019 IEEE PES Innovative Smart Grid Technologies Europe (ISGT-Europe)*, 2019, pp. 1–5.

[29] K. Nweye, B. Liu, P. Stone, and Z. Nagy, "Real-world challenges for multi-agent reinforcement learning in grid-interactive buildings," *Energy and AI*, vol. 10, p. 100202, 2022.

[30] D. Sandoval, P. Goffin, and H. Leibundgut, "How low exergy buildings and distributed electricity storage can contribute to flexibility within the demand side," *Applied Energy*, vol. 187, pp. 116–127, 2017.

[31] Y. Zhou and S. Cao, "Quantification of energy flexibility of residential net-zero-energy buildings involved with dynamic operations of hybrid energy storages and diversified energy conversion strategies," *Sustainable Energy, Grids and Networks*, vol. 21, p. 100304, 2020.

[32] J. Salpakari and P. Lund, "Optimal and rule-based control strategies for energy flexibility in buildings with pv," *Applied Energy*, vol. 161, pp. 425–436, 2016.

[33] R. Ruusu, S. Cao, B. Manrique Delgado, and A. Hasan, "Direct quantification of multiple-source energy flexibility in a residential building using a new model predictive high-level controller," *Energy Conversion and Management*, vol. 180, pp. 1109–1128, 2019.

[34] M. A. Judge, A. Khan, A. Manzoor, and H. A. Khattak, “Overview of smart grid implementation: Frameworks, impact, performance and challenges,” *Journal of Energy Storage*, vol. 49, p. 104056, 2022.

[35] Y. Fu, Z. O’Neill, Z. Yang, V. Adetola, J. Wen, L. Ren, T. Wagner, Q. Zhu, and T. Wu, “Modeling and evaluation of cyber-attacks on grid-interactive efficient buildings,” *Applied Energy*, vol. 303, p. 117639, 2021.

[36] P. Unahalekhaka and P. Sripakarach, “Reduction of reverse power flow using the appropriate size and installation position of a bess for a pv power plant,” *IEEE Access*, vol. 8, pp. 102 897–102 906, 2020.

[37] W. S. T. Fokui, M. Saulo, and L. Ngoo, “Controlled electric vehicle charging for reverse power flow correction in the distribution network with high photovoltaic penetration: case of an expanded ieee 13 node test network,” *Heliyon*, vol. 8, no. 3, 2022.

[38] J. Sánchez Ramos, M. Pavón Moreno, M. Guerrero Delgado, S. Álvarez Domínguez, and L. F. Cabeza, “Potential of energy flexible buildings: Evaluation of dsm strategies using building thermal mass,” *Energy and Buildings*, vol. 203, p. 109442, 2019.

[39] M. Pinamonti, A. Prada, and P. Baggio, “Rule-based control strategy to increase photovoltaic self-consumption of a modulating heat pump using water storages and building mass activation,” *Energies*, vol. 13, no. 23, p. 6282, 2020.

[40] N. Good, E. Karangelos, A. Navarro-Espinosa, and P. Mancarella, “Optimization under uncertainty of thermal storage-based flexible demand response with quantification of residential users’ discomfort,” *IEEE Transactions on Smart Grid*, vol. 6, no. 5, pp. 2333–2342, 2015.

[41] C. Fernández Bandera, J. Pachano, J. Salom, A. Peppas, and G. Ramos Ruiz, “Photovoltaic plant optimization to leverage electric self consumption by harnessing building thermal mass,” *Sustainability*, vol. 12, no. 2, p. 553, 2020.

[42] H. Wang, S. Riaz, and P. Mancarella, “Integrated techno-economic modeling, flexibility analysis, and business case assessment of an urban virtual power plant with multi-market co-optimization,” *Applied Energy*, vol. 259, p. 114142, 2020.

[43] A. Attarha, P. Scott, J. Iria, and S. Thiébaux, “Network-secure and price-elastic aggregator bidding in energy and reserve markets,” *IEEE Transactions on Smart Grid*, vol. 12, no. 3, pp. 2284–2294, 2021.

[44] I. Lampropoulos, G. M. Vanalme, and W. L. Kling, “A methodology for modeling the behavior of electricity prosumers within the smart grid,” in *Proc. Innovative Smart Grid Technologies Conference Europe (ISGT Europe)*, 2010, pp. 1–8.

[45] K. Clement-Nyns, E. Haesen, and J. Driesen, "The impact of charging plug-in hybrid electric vehicles on a residential distribution grid," *IEEE Transactions on Power Systems*, vol. 25, no. 1, pp. 371–380, 2010.

[46] I. Momber, A. Siddiqui, T. G. San Roman, and L. Söder, "Risk averse scheduling by a PEV aggregator under uncertainty," *IEEE Transactions on Power Systems*, vol. 30, no. 2, pp. 882–891, 2015.

[47] A. Sarker, Z. Li, W. Kolodzey, and H. Shen, "Opportunistic energy sharing between power grid and electric vehicles: A game theory-based nonlinear pricing policy," in *Proceedings of the 2017 IEEE 37th International Conference on Distributed Computing Systems (ICDCS)*, 2017, pp. 1197–1207.

[48] T. Cui, S. Chen, Y. Wang, S. Nazarian, and M. Pedram, "Optimal control of PEVs with a charging aggregator considering regulation service provisioning," *ACM Transactions on Cyber-Physical Systems*, vol. 1(4), no. 23, 2017.

[49] M. Wang, M. Ismail, R. Zhang, X. Shen, E. Serpedin, and K. Qaraqe, "Spatio-Temporal coordinated V2V energy swapping strategy for mobile PEVs," *IEEE Transactions on Smart Grid*, vol. 9, no. 3, pp. 1566–1579, 2018.

[50] N. Sadeghianpourhamami, N. Refa, M. Strobbe, and C. Develder, "Quantitive analysis of electric vehicle flexibility: A data-driven approach," *International Journal of Electrical Power & Energy Systems*, vol. 95, pp. 451–462, 2018.

[51] L. Chen and Z. Wu, "Study on the effect of ev charging to global load characteristics via charging aggregators," *Applied Energy Symposium and Forum, Renewable Energy Integration with Mini/Microgrids*, vol. 145, pp. 175–180, 2018.

[52] C. Luo, Y.-F. Huang, and V. Gupta, "Stochastic dynamic pricing for EV charging stations with renewable integration and energy storage," *IEEE Transactions on Smart Grid*, vol. 9, no. 2, pp. 1494–1505, 2018.

[53] D. Qiu, Y. Ye, D. Papadaskalopoulos, and G. Strbac, "A deep reinforcement learning method for pricing electric vehicles with discrete charging levels," *IEEE Transactions on Industry Applications*, vol. 56, no. 5, pp. 5901–5912, 2020.

[54] V. Moghaddam, A. Yazdani, H. Wang, D. Parlevliet, and F. Shahnia, "An online reinforcement learning approach for dynamic pricing of electric vehicle charging stations," *IEEE Access*, vol. 8, pp. 130 305–130 313, 2020.

[55] S. Wang, S. Bi, and Y. A. Zhang, "Reinforcement learning for real-time pricing and scheduling control in ev charging stations," *IEEE Transactions on Industrial Informatics*, vol. 17, no. 2, pp. 849–859, 2021.

[56] J. Li, X. Lin, S. Nazarian, and M. Pedram, "CTS2M: concurrent task scheduling and storage management for residential energy consumers under dynamic energy pricing," *IET Cyber-Physical Systems: Theory & Applications*, vol. 2, no. 3, pp. 111–117, 2017.

[57] D. Watari, I. Taniguchi, H. Goverde, P. Manganiello, E. Shirazi, F. Catthoor, and T. Onoye, "Multi-time scale energy management framework for smart PV systems mixing fast and slow dynamics," *Applied Energy*, vol. 289, no. 116671, 2021.

[58] T. Logenthiran, D. Srinivasan, and T. Z. Shun, "Demand side management in smart grid using heuristic optimization," *IEEE Transactions on Smart Grid*, vol. 3, no. 3, pp. 1244–1252, 2012.

[59] A.-H. Mohsenian-Rad and A. Leon-Garcia, "Optimal residential load control with price prediction in real-time electricity pricing environments," *IEEE Transactions on Smart Grid*, vol. 1, no. 2, pp. 120–133, 2010.

[60] C. Bennett, R. A. Stewart, and C. D. Beal, "Ann-based residential water end-use demand forecasting model," *Expert Systems with Applications*, vol. 40, no. 4, pp. 1014–1023, 2013.

[61] S. Rahman, M. G. Rabiul Alam, and M. Mahbubur Rahman, "Deep learning based ensemble method for household energy demand forecasting of smart home," in *2019 22nd International Conference on Computer and Information Technology (ICCIT)*, 2019, pp. 1–6.

[62] S. Sobri, S. Koohi-Kamali, and N. A. Rahim, "Solar photovoltaic generation forecasting methods: A review," *Energy Conversion and Management*, vol. 156, pp. 459–497, 2018.

[63] D. Anagnostos, T. Schmidt, S. Cavadias, D. Soudris, J. Poortmans, and F. Catthoor, "A method for detailed, short-term energy yield forecasting of photovoltaic installations," *Renewable Energy*, vol. 130, pp. 122–129, 2019.

[64] D. Watari, I. Taniguchi, and T. Onoye, "SoH aware battery management optimization on decentralized energy network," in *IEICE Transactions on Fundamentals of Electronics, Communications and Computer Sciences*, vol. 103, 2020, pp. 596–604.

[65] IBM, "IBM ILOG CPLEX Optimization Studio," http://www-03.ibm.com/software/products/ja/ibmilogcpleoptistud, [Online; accessed 9-Feb-2018].

[66] Ausgrid, "Electricity Usage Research," https://www.ausgrid.com.au/Industry/Our-Research/Data-to-share/Electricity-Research, [Online; accessed 25-Jan-2021].

[67] L. Pérez-Lombard, J. Ortiz, and C. Pout, “A review on buildings energy consumption information,” *Energy and Buildings*, vol. 40, no. 3, pp. 394–398, 2008.

[68] D. Watari, I. Taniguchi, H. Goverde, P. Manganiello, E. Shirazi, F. Catthoor, and T. Onoye, “Multi-time scale energy management framework for smart pv systems mixing fast and slow dynamics,” *Applied Energy*, vol. 289, p. 116671, 2021.

[69] D. Zhao, D. Watari, Y. Ozawa, I. Taniguchi, T. Suzuki, Y. Shimoda, and T. Onoye, “A thermal comfort and peak power demand aware vrf heating/cooling management framework: Simulation and on-site experiment,” *Journal of Information Processing*, vol. 30, pp. 476–485, 2022.

[70] Y. Yao and D. K. Shekhar, “State of the art review on model predictive control (mpc) in heating ventilation and air-conditioning (hvac) field,” *Building and Environment*, vol. 200, p. 107952, 2021.

[71] S. Taheri, P. Hosseini, and A. Razban, “Model predictive control of heating, ventilation, and air conditioning (hvac) systems: A state-of-the-art review,” *Journal of Building Engineering*, vol. 60, p. 105067, 2022.

[72] P. H. Shaikh, N. B. M. Nor, P. Nallagownden, I. Elamvazuthi, and T. Ibrahim, “A review on optimized control systems for building energy and comfort management of smart sustainable buildings,” *Renewable and Sustainable Energy Reviews*, vol. 34, pp. 409–429, 2014.

[73] M. Kasahara, T. Matsuba, Y. Kuzuu, T. Yamazaki, and e. al, “Design and tuning of robust pid controller for hvac systems,” *ASHRAE Transactions*, vol. 105, p. 154, 1999.

[74] Y.-G. Wang, Z.-G. Shi, and W.-J. Cai, “Pid autotuner and its application in hvac systems,” in *Proceedings of the 2001 American Control Conference. (Cat. No.01CH37148)*, vol. 3, 2001, pp. 2192–2196 vol.3.

[75] C. Dullinger, W. Struckl, and M. Kozek, “A general approach for mixed-integer predictive control of hvac systems using milp,” *Applied Thermal Engineering*, vol. 128, pp. 1646–1659, 2018.

[76] D. Zhao, D. Watari, Y. Ozawa, I. Taniguchi, T. Suzuki, Y. Shimoda, and T. Onoye, “Data-driven online energy management framework for hvac systems: An experimental study,” *Applied Energy*, vol. 352, p. 121921, 2023.

[77] F. Shen, L. Zhao, W. Du, W. Zhong, and F. Qian, “Large-scale industrial energy systems optimization under uncertainty: A data-driven robust optimization approach,” *Applied Energy*, vol. 259, p. 114199, 2020.

[78] X. Chen and N. Li, "Leveraging two-stage adaptive robust optimization for power flexibility aggregation," *IEEE Transactions on Smart Grid*, vol. 12, no. 5, pp. 3954–3965, 2021.

[79] Z. Li, L. Wu, Y. Xu, and X. Zheng, "Stochastic-weighted robust optimization based bilayer operation of a multi-energy building microgrid considering practical thermal loads and battery degradation," *IEEE Transactions on Sustainable Energy*, vol. 13, no. 2, pp. 668–682, 2022.

[80] H. Mansy and S. Kwon, "Optimal hvac control for demand response via chance-constrained two-stage stochastic program," *IEEE Transactions on Smart Grid*, vol. 12, no. 3, pp. 2188–2200, 2021.

[81] Y. Yang, G. Hu, and C. J. Spanos, "Stochastic optimal control of hvac system for energy-efficient buildings," *IEEE Transactions on Control Systems Technology*, vol. 30, no. 1, pp. 376–383, 2022.

[82] L. Zheng and L. Cai, "A distributed demand response control strategy using lyapunov optimization," *IEEE Transactions on Smart Grid*, vol. 5, no. 4, pp. 2075–2083, 2014.

[83] M. Cao, S. Chen, Z. Yang, and H. Miao, "Online optimization of heat pump systems for building heating based on lyapunov method," in *2022 IEEE Power & Energy Society Innovative Smart Grid Technologies Conference (ISGT)*, 2022, pp. 1–5.

[84] Z. Li, L. Wu, Y. Xu, S. Moazeni, and Z. Tang, "Multi-stage real-time operation of a multi-energy microgrid with electrical and thermal energy storage assets: A data-driven mpc-adp approach," *IEEE Transactions on Smart Grid*, vol. 13, no. 1, pp. 213–226, 2022.

[85] G. Serale, M. Fiorentini, A. Capozzoli, D. Bernardini, and A. Bemporad, "Model predictive control (mpc) for enhancing building and hvac system energy efficiency: Problem formulation, applications and opportunities," *Energies*, vol. 11, no. 3, p. 631, 2018.

[86] D. Zhao, D. Watari, Y. Ozawa, I. Taniguchi, T. Suzuki, Y. Shimoda, and T. Onoye, "A thermal comfort and peak power demand aware VRF heating/cooling management framework: Simulation and on-site experiment," *Journal of Information Processing*, vol. 30, pp. 476–485, 2022.

[87] F. Lopes, "Chapter 3 - from wholesale energy markets to local flexibility markets: structure, models and operation," in *Local Electricity Markets*, T. Pinto, Z. Vale, and S. Widergren, Eds. Academic Press, 2021, pp. 37–61.

[88] L. Tschora, E. Pierre, M. Plantevit, and C. Robardet, "Electricity price forecasting on the day-ahead market using machine learning," *Applied Energy*, vol. 313, p. 118752, 2022.

[89] V. Sridharan, M. Tuo, and X. Li, "Wholesale electricity price forecasting using integrated long-term recurrent convolutional network model," *Energies*, vol. 15, no. 20, p. 7606, 2022.

[90] K. Iwabuchi, K. Kato, D. Watari, I. Taniguchi, F. Catthoor, E. Shirazi, and T. Onoye, "Flexible electricity price forecasting by switching mother wavelets based on wavelet transform and long short-term memory," *Energy and AI*, vol. 10, p. 100192, 2022.

[91] S. Zhou, L. Zhou, M. Mao, H.-M. Tai, and Y. Wan, "An optimized heterogeneous structure lstm network for electricity price forecasting," *IEEE Access*, vol. PP, pp. 1–1, 2019.

[92] U. Ugurlu, I. Oksuz, and O. Tas, "Electricity price forecasting using recurrent neural networks," *Energies*, vol. 11, no. 5, p. 1255, 2018.

[93] J. Naughton, H. Wang, M. Cantoni, and P. Mancarella, "Co-optimizing virtual power plant services under uncertainty: A robust scheduling and receding horizon dispatch approach," *IEEE Transactions on Power Systems*, vol. 36, no. 5, pp. 3960–3972, 2021.

[94] G. Tsaousoglou, J. S. Giraldo, and N. G. Paterakis, "Market mechanisms for local electricity markets: A review of models, solution concepts and algorithmic techniques," *Renewable and Sustainable Energy Reviews*, vol. 156, p. 111890, 2022.

[95] J. Gilmore, T. Nolan, and P. Simshauser, *The Levelised Cost of Frequency Control Ancillary Services in Australia's National Electricity Market*, 2022.

[96] Australian Energy Market Operator (AEMO), "Aemo | pre-dispatch," https://aemo.com.au/energy-systems/electricity/national-electricity-market-nem/data-nem/market-management-system-mms-data/pre-dispatch, accessed: 2023-1-19.

[97] I. E. Agency, "Net Zero by 2050 A Roadmap for the Global Energy Sector," https://iea.blob.core.windows.net/assets/deebef5d-0c34-4539-9d0c-10b13d840027/NetZeroby2050-ARoadmapfortheGlobalEnergySector_CORR.pdf, [Online; accessed 29-Dec-2023].

[98] IRENA, "FUTURE OF SOLAR PHOTOVOLTAIC ," https://www.irena.org/-/media/Files/IRENA/Agency/Publication/2019/Nov/IRENA_Future_of_Solar_PV_2019.pdf, [Online; accessed 22-Nov-2023].

[99] U. D. of Energy's National Renewable Energy Laboratory, "Rooftop Solar Photovoltaic Technical Potential in the United States: A Detailed Assessment," https://www.nrel.gov/docs/fy16osti/65298.pdf, [Online; accessed 22-Nov-2023].

[100] I. E. Agency, "Demand Response," https://www.iea.org/energy-system/energy-efficiency-and-demand/demand-response, [Online; accessed 29-Dec-2023].